

Aus der Klinik und Poliklinik für Radiologie
der Ludwig-Maximilians-Universität München
Direktor: Prof. Dr. med. Jens Ricke

Untersuchungen zur Rolle der Ganzhirn CT-Perfusion in der akuten
Schlaganfalldiagnostik

Dissertation
zum Erwerb des Doktorgrades der Medizin
an der Medizinischen Fakultät der
Ludwig-Maximilians-Universität zu München

vorgelegt von
Christine Bollwein
aus Schwandorf
2018

Mit Genehmigung der Medizinischen Fakultät
der Universität München

Berichterstatter: Prof. Dr. med. Wieland Sommer, MPH

Mitberichterstatter: Prof. Dr. Michael Ewers
Prof. Dr. Roman Haberl
PD Dr. Manfred Uhr

Mitbetreuung durch die
promovierten Mitarbeiter: PD Dr. med. Louisa von Baumgarten
PD Dr. med. Dipl. Wirt.-Inform. Kolja Thierfelder

Dekan: Prof. Dr. med. dent. Reinhard Hickel

Tag der mündlichen Prüfung: 22.03.2018

Vorwort

Während meiner Doktorandentätigkeit unter Betreuung von Prof. Dr. Wieland Sommer, PD Dr. med. Louisa von Baumgarten und PD Dr. med. Dipl. Wirt.-Inform. Kolja Thierfelder sind folgende wissenschaftliche Artikel unter meiner Mitwirkung entstanden:

Originalarbeiten:

Diagnostic accuracy of whole-brain CT perfusion in the detection of acute infratentorial infarctions

Christine Bollwein*, Annika Plate, Wieland H. Sommer, Kolja M. Thierfelder, Hendrik Janssen, Maximilian F. Reiser, Andreas Straube, Louisa von Baumgarten

Neuroradiology. 2016 Nov; 58(11):1077-1085

Impact factor 2016: 2,3

* geteilte Erstautorenschaft

Crossed cerebellar diaschisis in patients with acute middle cerebral artery infarction: Occurrence and perfusion characteristics

Wieland H Sommer, **Christine Bollwein***, Kolja M Thierfelder, Alena Baumann, Hendrik Janssen, Birgit Ertl-Wagner, Maximilian F. Reiser, Annika Plate, Andreas Straube, Louisa von Baumgarten

J Cereb Blood Flow Metab. 2016 Apr; 36(4):743-54

Impact factor 2016: 4,9

* geteilte Erstautorenschaft

Early CT perfusion mismatch in acute stroke is not time-dependent but relies on collateralization grade

Louisa von Baumgarten, Kolja M. Thierfelder, Sebastian E. Beyer, Alena B. Baumann, **Christine Bollwein**, Hendrik Janssen, Maximilian F. Reiser, Andreas Straube, Wieland H. Sommer

Neuroradiology. 2016 Apr; 58(4):357-65

Impact factor 2016: 2,3

Kumulative Dissertation gemäß §4a der Promotionsordnung

Inhaltsverzeichnis

I	Einleitung	5
I.1	Ischämischer Schlaganfall	5
I.1.1	Epidemiologische Kenndaten	5
I.1.2	Pathophysiologie des ischämischen Schlaganfalls	5
I.1.3	Therapie des ischämischen Schlaganfalls.....	5
I.2	CT-Perfusion in der Schlaganfalldiagnostik.....	7
I.2.1	Methodische Grundlagen der CT-Perfusion.....	7
I.2.2	Darstellung pathophysiologischer Veränderungen mittels CT-Perfusion	9
I.3	Zielsetzung der vorliegenden Forschungsarbeiten	10
II	Orginalarbeiten	12
II.1	Diagnostische Verlässlichkeit der Ganzhirn CT-Perfusion in der Detektion von akuten infratentoriellen Schlaganfällen	12
II.2	Gekreuzte zerebelläre Diaschisis bei Patienten mit akutem Infarkt der Arteria cerebri media: Vorkommen und Perfusionsmerkmale.....	13
II.3	Der „mismatch“ in den unterschiedlichen CT-Perfusionskarten beim akuten Schlaganfall hängt nicht von der Zeit nach Einsetzen der Ischämie sondern vom Grad der Kollateralisierung ab	15
III	Zusammenfassung/Summary	16
IV	Literaturverzeichnis	19
V	Veröffentlichungen	23
V.1	Diagnostic accuracy of whole-brain CT perfusion in the detection of acute infratentorial infarctions	23
V.2	Crossed cerebellar diaschisis in patients with acute middle cerebral artery infarction: occurrence and perfusion characteristics.....	33
V.3	Early CT perfusion mismatch in acute stroke is not time-dependent but relies on collateralization grade	46
VI	Lebenslauf	56
VII	Danksagung	57
VIII	Eidesstattliche Versicherung	58

I Einleitung

I.1 Ischämischer Schlaganfall

I.1.1 Epidemiologische Kenndaten

Nach Angaben der *World Stroke Organization* erleiden weltweit jährlich 15 Millionen Menschen einen Schlaganfall. Konkret bedeutet dies, dass jeder sechste Mensch in seinem Leben von einem Schlaganfall betroffen sein wird.¹ Dieses Krankheitsbild stellt zudem weltweit die zweithäufigste Todesursache dar. Der Schlaganfall ist einer der führenden Gründe für Behinderung und frühzeitige Invalidität und dadurch ein wesentlicher Kostenfaktor für Gesundheitssysteme.²⁻⁵ In Deutschland ereignen sich etwa 200.000 Neuerkrankungen pro Jahr. Der Schlaganfall ist somit die häufigste neurologische Erkrankung in der Bundesrepublik Deutschland.⁶

I.1.2 Pathophysiologie des ischämischen Schlaganfalls

In 87% der Fälle liegt ein ischämischer Schlaganfall vor, der durch lokale arteriosklerotische Veränderungen (mikro- oder makroangiopathisch) oder durch embolische (thromb- oder kardioembolisch) Geschehnisse bedingt ist.⁷ Dabei kommt es zu einer regionalen Minderperfusion und Hypoxie des nachgeschalteten Hirnareals. Neurologisch äußert sich dieser Defekt als fokales neurologisches Defizit. Das irreversibel geschädigte Hirnparenchym mit Zelluntergang bildet den Infarktkern, der von einer Zone aus minderversorgtem aber potentiell rettbarem Gewebe, der sogenannten Penumbra, umgeben ist.⁸ Die Neurone der Penumbra sind durch den relativen Sauerstoffmangel geschädigt, funktionell jedoch noch intakt.^{9, 10} Entscheidend für das Outcome nach einem Schlaganfall ist der Erhalt der Vitalität der Penumbra. Erreicht wird dies durch eine frühestmögliche Reperfusionstherapie, die verhindert, dass sich der Infarktkern auf die minderperfundierte Penumbra ausdehnt.¹¹ Man nimmt an, dass die Expansion des Infarktkerns proportional zur Anfälligkeit des Gewebes für Hypoxie, zum Schweregrad der Hypoperfusion und zur verstrichenen Zeit nach Einsetzen der Ischämie ist.¹² Mit zeitnaher Reperfusion kann somit die Penumbra vor dem Zerfall bewahrt werden, was letztendlich zu einem verbesserten neurologischen Outcome führt.¹³

I.1.3 Therapie des ischämischen Schlaganfalls

Zur Thrombolyse stehen zwei verschiedene Verfahren zur Verfügung. Zum einen besteht die Möglichkeit der systemischen Lyse durch intravenöse (i. v.) Applikation des Fibrinolytikums rekombinanter Gewebeplasminogenaktivator (recombinant tissue plasminogen activator,

rtPA). Diese Therapieform wurde bereits 1995 eingeführt und stellte für zwei Jahrzehnte die einzige kausale Behandlungsmöglichkeit mit bewiesener Wirksamkeit dar. Sie sollte gemäß der aktuellen Leitlinien der Fachgesellschaften innerhalb eines Zeitfensters von 4,5 Stunden nach Symptombeginn erfolgen.¹¹ Dies hat den Hintergrund, dass eine Zeitverzögerung über dieses Zeitfenster hinaus nicht nur zu einer Abnahme der Effektivität der Lysetherapie sondern auch zu einem erhöhten Risiko für eine sekundäre Einblutung in die infarzierte Region führt.¹⁴⁻¹⁶ Diese tritt bei bis zu 6,1% der behandelten Schlaganfallpatienten auf und verschlechtert die Prognose signifikant.¹⁷ Das enge Zeitfenster hat jedoch zur Folge, dass weniger als 10% der Patienten eine thrombolytische Therapie erhalten.¹⁸

Zum anderen kann, alternativ zur systemischen Lyse, eine kathetergestützte endovaskuläre Intervention in Form einer lokalen intraarteriellen Fibrinolyse oder einer mechanischen Thrombektomie das Outcome von Schlaganfallpatienten mit einem proximalen Verschluss der hirnversorgenden Arterien verbessern.¹¹ Die mechanische Thrombektomie, insbesondere mittels eines sogenannten „stent retrievers“, hat sich als sicheres und effektives Verfahren zur Behandlung von Verschlüssen großer Arterien der vorderen Strombahn erwiesen.¹⁹⁻²¹ Die endovaskuläre Therapie wird daher von der *American Heart Association* zu den größten zehn Forschungserfolgen auf dem Gebiet der kardiovaskulären Erkrankungen gezählt.²²

Die Erfolgsaussicht einer Reperfusionstherapie steigt, je kürzer das Zeitfenster zwischen Symptom- und Therapiebeginn gehalten werden kann. Oftmals ist der Symptombeginn jedoch nicht eruierbar (insbesondere bei Schlaganfällen, die sich im Schlaf ereignen)^{23, 24} oder die Zeitgrenze von 4,5 Stunden bereits überschritten. Dies hat zur Folge, dass nur etwa 6% der Schlaganfallpatienten, die innerhalb von drei Stunden in die Klinik eingeliefert werden, eine Fibrinolysetherapie erhalten. Die Erweiterung des Zeitfensters von 3 Stunden (festgelegter Grenzwert bis 2015) auf 4,5 Stunden²⁵ führte lediglich zu einer Zunahme der Fibrinolyserate um 0,5%.²⁶

Im Fokus des aktuellen Interesses steht die Frage, ob es Patienten gibt, die stärker oder auch über das enge Zeitfenster hinaus von einer therapeutischen Intervention profitieren. Da der wesentliche therapeutische Angriffspunkt der Erhalt der Penumbra ist, wäre es denkbar, dass dies auf Patienten mit einer großen Penumbra und folglich einem großen „mismatch“ („Nichtübereinstimmen“) zwischen dem gesamten perfusionsgestörten Hirngewebe und dem Infarktkern zutrifft. Tatsächlich zeigen erste Studien, dass die bildgestützte Auswahl von Patienten mit einer, in Relation zum Infarktkern, großen Penumbra einen Benefit in der Nutzen-Risiko-Bewertung eines verlängerten therapeutischen Zeitfensters besitzt.^{27, 28}

Sowohl Infarktkern als auch Penumbra kommen unter anderem in der CT-Perfusion (computed tomography perfusion, CTP) zur Darstellung.²⁹

I.2 CT-Perfusion in der Schlaganfalldiagnostik

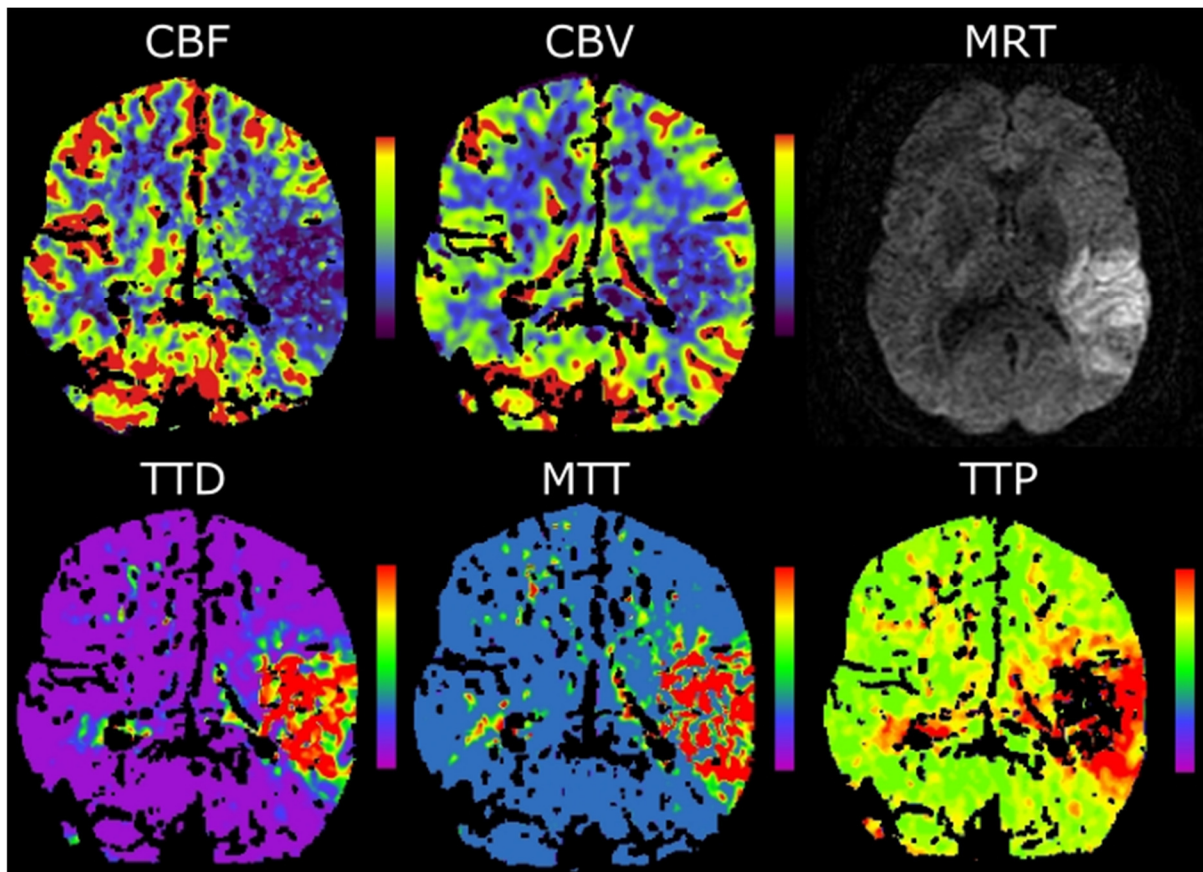
I.2.1 Methodische Grundlagen der CT-Perfusion

Die Anfänge der CT-Perfusion (CTP) reichen zurück bis in das Jahr 1980. Damals veröffentlichte *Leon Axel* erste theoretische Überlegungen zur Bestimmung der Gewebepfusion anhand dynamischer, mittels Kontrastmittel gewonnener CT Daten.³⁰ Zunächst blieb dieses neuartige bildgebende Verfahren auf Forschungsarbeiten beschränkt, da hierfür eine rasche Bildaufnahme und –verarbeitung erforderlich sind. Mit dem Aufkommen der Mehrschicht-Spiral-CT konnte jedoch die Datenerfassung und –verarbeitung enorm beschleunigt und somit die Anwendbarkeit der CTP außerhalb von Studien ermöglicht werden.^{31, 32} Zudem erleichterte die Einführung kommerzieller Softwarepakete zur Datenakquise und -verarbeitung den Einzug dieser Technik in den klinischen Alltag. Heutzutage stellt die CTP in den meisten Schlaganfallzentren neben dem Nativ-CT und der CT-Angiographie einen wesentlichen Bestandteil in der Akutdiagnostik zerebrovaskulärer Ereignisse dar.³³

Die Theorie der CTP beruht auf dem sogenannten „central volume principle“. Die Parameter CBF (cerebral blood flow; gesamtes Blutvolumen, das in einer bestimmten Zeit durch eine definierte Parenchymmasse fließt; ml/(min*100 g)), CBV (cerebral blood volume; gesamtes Blutvolumen innerhalb einer Parenchymmasse; ml/100 g) und MTT (mean transit time; durchschnittliche Passagezeit des Kontrastmittelbolus durch ein bestimmtes Parenchymvolumen; Sekunden) stehen dabei im folgendem Zusammenhang: $CBF = CBV/MTT$. Für die Berechnung der Perfusionsparameter ist die intravenöse Applikation eines iodierten Kontrastmittelbolus nötig, dessen initiale Passage durch das zerebrale Gefäßbett anhand wiederholter Aufnahmen über die Zeit verfolgt wird. Aufgrund der linearen Beziehung zwischen der Kontrastmittelkonzentration und der Abschwächung der Röntgenstrahlung können Konzentrations-Zeit-Kurven für das arterielle Zuflussgefäß (AIF; arterial input function), das venöse Abflussgefäß (VOF; venous output function) sowie für jedes Pixel des Hirnparenchyms aufgezeichnet werden.^{29, 34, 35}

Dekonvolutions- und Nicht-Dekonvolutions-basierte Modellansätze nutzen die erhaltenen Funktionen zur Bestimmung der mittleren Durchflusszeit MTT und des zerebralen

Blutvolumens CBV.³⁵ Aus der oben genannten Gleichung lässt sich letztendlich der zerebrale Blutfluss CBF bestimmen. Neuere Indizes zur Charakterisierung der Hirnperfusion umfassen die TTD (time to drain; Dauer des Kontrastmittel-washouts; Sekunden) und die TTP (time to peak; Zeitintervall zwischen Kontrastmittelinjektion und maximaler Kontrastmittelkonzentration; Sekunden). Zur anschaulichen Darstellung der Perfusionsparameter werden zusätzlich farbcodierte Schnittbilder (maps) erzeugt, die die Grundlage der Routinebefundung bilden (siehe Abbildung).



Schlaganfallbildgebung mittels Ganzhirn CTP und MRT

Repräsentative Bildbeispiele eines 35-jährigen Patienten mit einer globalen Aphasie, einer Hemiparese rechts und einem sensiblen Neglect bei akutem Infarkt der Arteria cerebri media links. Die Genese ist am ehesten arterio-arteriell embolisch bei Dissektion der A. carotis interna links bedingt. Aufgrund des unklaren Zeitfensters konnte keine Lysetherapie durchgeführt werden.

Dargestellt sind die CTP Sequenzen CBF (cerebral blood flow), CBV (cerebral blood volume), TTD (time to drain), MTT (mean transit time) und TTP (time to peak) sowie die Verlaufskernspintomographie (MRT-DWI, diffusion weighted imaging).

Die initiale CTP Bildgebung zeigt im linken Mediaterritorium einen Unterschied (engl. „mismatch“) in der Ausdehnung des Perfusionsdefizites in den Sequenzen CBF, TTD, MTT, TTP im Vergleich mit der Sequenz CBV. Der in der Verlaufskernspintomographie zur Darstellung kommende Infarkt umfasst nicht die maximale Ausdehnung des initialen Perfusionsdefizites, sondern in erster Linie das Areal, welches sowohl ein Perfusionsdefizit in den Sequenzen CBF, TTD, MTT, TTP als auch in der Sequenz CBV aufwies (engl. „match“).

I.2.2 Darstellung pathophysiologischer Veränderungen mittels CT-Perfusion

Den höchsten Stellenwert nimmt die CTP in der Diagnostik von ischämischen Schlaganfällen ein. Vor Etablierung der CTP und CT-Angiographie in der Akutdiagnostik bei Verdacht auf einen Schlaganfall stand lediglich die konventionelle Nativ-CT (keine Kontrastmittelapplikation) zur Verfügung. Während die Nativ-CT immer noch ihre Berechtigung im Ausschluss einer intrakraniellen Blutung hat, ist ihre Verlässlichkeit in der Erkennung von frühen ischämischen Veränderungen anhand von sogenannten Infarktfrühzeichen wie dem hyperdensen Mediazeichen, dem Verstreichen des Sulcusreliefs und der Aufhebung der Mark-Rinden-Grenze vergleichsweise gering.³⁶ Die CT-Perfusion erhöht die Treffsicherheit in der Diagnosestellung eines ischämischen Schlaganfalls deutlich.³⁷ Zudem liefert die CT-Perfusion zusätzliche Informationen über pathophysiologische Aspekte wie zum Beispiel das größenmäßige Verhältnis von Infarktkern zu Penumbra.

Pathophysiologisch liegt den Perfusionsverhältnissen in dem Infarktkern bzw. in der Penumbra die zerebrovaskuläre Autoregulation zugrunde. Durch die Abnahme des Perfusionsdrucks im Rahmen eines Gefäßverschlusses kommt es sowohl im Infarktkern als auch in der Penumbra zu einer Verlängerung der MTT. Im Gegensatz zum Infarktkern, wo die Autoregulation nicht mehr funktioniert und das CBV und der CBF abfallen, findet in der Penumbra eine kompensatorische Vasodilatation statt, die zu einem Erhalt des CBV führt.³⁸

Die Diskrepanz zwischen den Hirnvolumina mit erhaltenem/erhöhtem CBV und vermindertem CBV bei reduziertem CBF bzw. verlängerter MTT bezeichnet man als „mismatch“ (siehe Abbildung). Dies spiegelt die Penumbra wider. Im Gegensatz dazu kennzeichnet den Infarktkern ein Hirnvolumen mit einer Übereinstimmung, also einem „match“, der Perfusionsparameter in Form einer verlängerten MTT, eines reduzierten CBF sowie eines verminderten CBV. In jüngster Zeit wurde das Spektrum der Perfusionsparameter um die TTD und TTP erweitert. Während sich die TTD als sehr sensitiv in der Detektion von minderperfundierten Arealen erweist, ist die TTP durch ihre Abhängigkeit von externen Faktoren wie z. B. extra- und intrakraniellen Stenosen fehlerbelastet.^{39, 40} Patienten mit einer im Vergleich zum Infarktkern großen Penumbra scheinen besonders von einer thrombolytischen Therapie zu profitieren, weswegen die Perfusionsbildgebung eingesetzt wird, um Patienten zu identifizieren, die von einer Therapie innerhalb eines erweiterten Zeitfensters (für die systemische Lyse innerhalb von sechs Stunden und für die mechanische Thrombektomie mehr

als sechs Stunden nach Symptombeginn) profitieren.⁴¹ Die bildgestützte Patientenselektion wird bisher jedoch vor allem in klinischen Studien angewendet.

Bisher herrscht in der Literatur keine Einigkeit darüber, wie die Penumbra bzw. der Infarktkern anhand der Perfusionsparameter quantitativ erfasst werden soll.⁴² Diese mangelnde Standardisierung beruht unter anderem darauf, dass die CT-Perfusion mit unterschiedlichen Akquisitionsparametern, verschiedenen Analyse- und Berechnungsmethoden und unterschiedlichen Softwarepaketen zur Auswertung erfasst wird.

Im klinischen Alltag wird das Ausmaß des „mismatches“ meist rein visuell beurteilt. Die softwaregestützte Volumetrie der „mismatch“-Ausdehnung ist zwar zeitaufwändiger, jedoch verlässlicher und erreicht eine bessere Reproduzierbarkeit der Ergebnisse⁴³.

Ein entscheidender Nachteil der CTP war lange Zeit ihre eingeschränkte Erfassung des Hirnparenchyms in kraniokaudaler Richtung. Die Standard CTP war typischerweise auf zwei axiale Schichten auf Höhe der Basalganglien und ein bis zwei Zentimeter darüber beschränkt. Technische Entwicklungen wie die Erhöhung der Zahl an Detektorzeilen, das Spiralverfahren und die sogenannte „toggling-table“-Technik (hierbei nimmt der Untersuchungstisch abwechselnd zwei Positionen ein, um die räumliche Abdeckung zu verdoppeln) ermöglichen eine Erweiterung der Scanweite auf nahezu das gesamte Gehirnvolumen in der Z-Achse (kranio-kaudale Ausdehnung)^{44, 45}. Somit kann nun auch die hintere Schädelgrube durch die CTP abgebildet werden. Daten zur diagnostischen Wertigkeit dieser Bildgebungsmodalität in der hinteren Strombahn liegen jedoch kaum vor. In einer Fülle von Studien wird die CTP als verlässlich, akkurat und praktikabel beschrieben. Diese Studien beziehen sich jedoch fast ausschließlich auf supratentorielle Infarkte.⁴⁶

I.3 Zielsetzung der vorliegenden Forschungsarbeiten

Im Rahmen der vorliegenden Forschungsarbeiten wurde aus einem Kollektiv von bis zu 1644 Patienten, die im Kontext der akuten Schlaganfallversorgung zwischen dem 29.03.2009 und dem 12.12.2014 eine multimodale Ganzhirn CT-Untersuchung erhalten hatten, verschiedene Studienpopulationen gebildet und hinsichtlich unterschiedlicher Fragestellungen analysiert.

- 1) In einem ersten Projekt wurde die diagnostische Verlässlichkeit der Ganzhirn CT-Perfusion in der Detektion von akuten infratentoriellen Schlaganfällen evaluiert.

- 2) Das Ziel der Folgestudie war, das Auftreten einer zerebellären Perfusionsänderung nach akuten supratentoriellen Infarkten im Rahmen der zerebellären Diaschisis zu analysieren.
- 3) In der letzten Studie wurde untersucht, welche Determinanten das Ausmaß des initialen „mismatches“ in der CTP bestimmen.

II Originalarbeiten

II.1 Diagnostische Verlässlichkeit der Ganzhirn CT-Perfusion in der Detektion von akuten infratentoriellen Schlaganfällen

Ziel der Fall-Kontroll-Studie war es, die Sensitivität und Spezifität der CTP für infratentorielle Infarkte zu ermitteln. Aus einem Kollektiv von 1380 Patienten, die im Rahmen der akuten Schlaganfallversorgung eine multimodale CT Bildgebung erhalten hatten, wurden retrospektiv 70 Fälle mit einer (durch MRT bestätigten) infratentoriellen ischämischen Läsion identifiziert und Kontrollen ohne Infarkt im hinteren Stromgebiet gegenübergestellt. Die entsprechenden Perfusionsmaps wurden von zwei unabhängigen, verblindeten Befundern hinsichtlich dem Vorhandensein und der Lokalisation eines ischämischen Infarkts ausgewertet.

Allgemein erzielte die CTP anhand der gewonnenen Ergebnisse eine Sensitivität von 41,4% und eine Spezifität von 93,3% in der Diagnose infratentorieller Infarkte. Die Parameter MTT und TTD erwiesen sich dabei als am sensitivsten und der Parameter CBV als am spezifischsten. Entscheidenden Einfluss auf die korrekte Befundung hatte die Größe des Infarktes, wobei kleine Infarkte mit einem Durchmesser unter 19mm nur in ca. 20% der Fälle korrekt identifiziert wurden. Im Gegensatz dazu erreichte die CTP bei Infarkten mit einem Durchmesser über 19mm eine Sensitivität von 60%. Außerdem spielte die Lokalisation der Infarkte eine Rolle für die korrekte Diagnose: Läsionen im Hirnstamm wurden weniger häufig korrekt identifiziert als im Kleinhirn. Die Spezifität ist sowohl für supra- als auch für infratentorielle Ischämien vergleichbar. Ähnlich wie auch hier gezeigt reduziert sich die Sensitivität supratentorieller Infarkte, sobald sie sich subkortikal befinden und nur eine geringe Größe erreichen („lakunäre“ Infarkte).^{39, 47, 48}

Der Beitrag zu dieser Publikation umfasste die retrospektive Auswahl des Studienkollektivs, die Aufbereitung und statistische Analyse der Ergebnisse sowie das Verfassen des Manuskripts.

Die Arbeit wurde in *Neuroradiology* mit einem impact factor von 2,3 publiziert.

II.2 Gekreuzte zerebelläre Diaschisis bei Patienten mit akutem Infarkt der Arteria cerebri media: Vorkommen und Perfusionsmerkmale

Als gekreuzte zerebelläre Diaschisis (im angloamerikanischen Raum als „crossed cerebellar diaschisis“ bezeichnet, CCD) wird eine Abnahme der Stoffwechselaktivität und der Perfusion in der kontralateral zu einer supratentoriellen Schädigung gelegenen Kleinhirnhemisphäre bezeichnet. Diese wurde unter anderem nach ischämischen Infarkten, Hirnblutungen, epileptischen Anfällen und Hirntumoren des Großhirns beschrieben.⁴⁹⁻⁵³ Relevante pathophysiologische Aspekte der CCD nach ischämischen Infarkten wie deren Auftretenswahrscheinlichkeit, ihr prognostischer Wert, ihr klinisches Korrelat und ihre Abhängigkeit von Lokalisation und Ausmaß des supratentoriellen Schadens sind nur unzureichend erforscht. Die Ganzhirn CTP ermöglicht prinzipiell die Kleinhirnperfusion abzubilden und stellt somit ein geeignetes Verfahren dar, die CCD nach einem akuten Schlaganfall an einem großen Patientenkollektiv zu untersuchen. In der vorliegenden Publikation wurde daher die Häufigkeit einer CCD nach akuten Infarkten der Arteria cerebri media (MCA) bestimmt und mögliche Einflussfaktoren auf deren Auftretenswahrscheinlichkeit identifiziert. Hierzu wurden im Rahmen einer Fall-Kontroll-Studie aus einem Kollektiv von 1644 Patienten 156 Patienten mit einem akuten Infarkt im MCA-Stromgebiet identifiziert und 352 Kontrollpatienten ohne Infarkt gegenübergestellt. Eine CCD konnte bei 35,3% der Patienten mit akutem Mediainfarkt beobachtet werden. Einen signifikanten Einfluss auf das Vorkommen der CCD hatte die Infarktlokalisierung. Infarkte, die in der linken Hemisphäre lokalisiert waren und den Frontallappen in das Infarktareal miteinbezogen, waren mit dem Auftreten einer CCD assoziiert. Basierend auf den Perfusionsparametern MTT, TTD und CBF zeigte sich eine positive Korrelation zwischen dem Ausmaß der supratentoriellen Perfusionseinschränkung und der Auftretenswahrscheinlichkeit der CCD. Eine Korrelation zwischen dem Grad der supratentoriellen Perfusionsstörung und der Intensität der zerebellären Minderperfusion bestand jedoch nicht. Auch andere patientenbezogene Faktoren wie Alter oder Geschlecht hatten keinen Einfluss auf die Auftretenswahrscheinlichkeit einer CCD.

Zusammenfassend konnte gezeigt werden, dass die CCD ein verbreitetes Phänomen nach einem akuten Infarkt der MCA ist und verlässlich mithilfe der CTP nachgewiesen werden kann. Zudem scheint die Infarktlokalisierung und das Ausmaß der Perfusionsabnahme eine größere Rolle im Entstehen der CCD zu spielen als das reine Infarktvolumen. In Anbetracht der Häufigkeit der CCD ist es für jeden Befunder von CTP-Bildern wichtig, dass Vorkommen der

CCD nach supratentoriellen Infarkten zu berücksichtigen, um kontralaterale zerebelläre Perfusionsdefizite korrekt zu klassifizieren.

Die Erhebung des Studienkollektivs, die Aufarbeitung der CT-Bilder, die statistische Auswertung der Daten sowie die Erstellung der Tabellen und das Verfassen des Manuskripts gehören zu den Beiträgen, die mit dieser Publikation verbunden waren.

Die Arbeit wurde im *Journal of Cerebral Blood Flow and Metabolism* mit einem impact factor von 4,9 publiziert.

II.3 Der „mismatch“ in den unterschiedlichen CT-Perfusionskarten beim akuten Schlaganfall hängt nicht von der Zeit nach Einsetzen der Ischämie sondern vom Grad der Kollateralisation ab

Die Penumbra stellt die entscheidende Zielstruktur der therapeutischen Intervention beim Schlaganfall dar. Die wesentlichen Determinanten, die das Ausmaß der Penumbra bestimmen, insbesondere die Rolle des Zeitraumes nach Symptombeginn, sind nicht abschließend geklärt.

Das Ziel der retrospektiven Studie war es daher, in einem relevanten Patientenkollektiv den Einfluss der Zeit nach Einsetzen der Ischämie, der Lokalisation des Gefäßverschlusses und des Grades der leptomeningealen Kollateralisierung auf das Ausmaß des „mismatches“ zwischen CBV und CBF als Maß für die Penumbra nach einem akuten Mediainfarkt zu bestimmen.

Aus einem Kollektiv von 992 konsekutiv untersuchten Patienten, die unter der Verdachtsdiagnose eines Schlaganfalles in der radiologischen Abteilung des Universitätsklinikums Großhadern untersucht wurden, konnten 103 Patienten, bei denen der Zeitpunkt bei Auftreten der Symptome bekannt war, das initiale CBF Volumen mehr als 10 ml betrug und die einen in der Follow-up MRT bestätigten Infarkt der Arteria cerebri media aufwiesen, in die Studie eingeschlossen werden.

Die univariate bzw. multivariate Analyse ergab, dass die Zeit nach Symptombeginn nicht mit dem relativen oder absoluten „mismatch“ korrelierte. Ein höherer Kollateralisierungsgrad sowie ein Verschluss der Arteria carotis interna hingegen waren mit einem kleinen bzw. großen „mismatch“ assoziiert.

Somit unterstreichen die Ergebnisse den Einfluss der individuell unterschiedlich ausgebildeten leptomeningealen Kollateralen sowie der Verschlusslokalisierung auf das Ausmaß und die Zusammensetzung der ischämischen Region, wohingegen die Zeit nach Symptombeginn eine eher untergeordnete Rolle spielt.

Der Arbeitsaufwand zu dieser Veröffentlichung bestand in der Bewertung der Daten vor dem Hintergrund der aktuellen Literatur, einer ausführlichen Literaturrecherche und in der Mitarbeit beim Verfassen des Manuskripts.

Die Arbeit wurde in *Neuroradiology* mit einem impact factor von 2,3 publiziert.

III Zusammenfassung/Summary

Zusammenfassung

Die Einführung der Ganzhirn CTP ermöglicht es, Einblicke in die pathophysiologischen Veränderungen bei zerebralen Durchblutungsstörungen im Rahmen des akuten Schlaganfalls zu gewinnen. In der vorliegenden Promotion wurden drei Studien zur Rolle der Ganzhirn-CTP im Rahmen der Schlaganfalldiagnostik durchgeführt.

I) Durch die Ausdehnung der Scanweite in der Z-Achse ist seit kurzem die hintere Schädelgrube der Routinebildgebung zugänglich. Somit können infratentorielle Perfusionsalterationen dargestellt werden. In der ersten Studie wurde die diagnostische Wertigkeit der Ganzhirn CT-Perfusion in der Detektion von infratentoriellen Infarkten untersucht.

II) Die CCD („crossed cerebellar diaschisis“) bezeichnet eine Reduktion des Blutflusses und der Stoffwechselaktivität in der Kleinhirnhälfte, die sich kontralateral zur geschädigten Großhirnhälfte befindet. In der zweiten Studie wurden die Häufigkeit sowie die Charakteristika der CCD nach akuten Infarkten im Versorgungsgebiet der Arteria cerebri media untersucht.

III) Zielsetzung der dritten Studie war es, Faktoren zu ermitteln, die Einfluss auf das Ausmaß der Penumbra haben. Im Gegensatz zum Infarktkern kann die strukturell erhaltene Penumbra durch therapeutische Intervention vor dem Übergang in irreversibel geschädigtes Hirnparenchym bewahrt werden. Kenntnisse über die patientenspezifische Zusammensetzung des Infarktareals in Penumbra und Infarktkern auf der Basis der Ganzhirn CTP eröffnen die Möglichkeit von individuell angepassten Therapieentscheidungen.

Zusammenfassend können folgende Kernaussagen getroffen werden:

I) Mit einer Spezifität von 93,3% und einer Sensitivität von 41,4% ist die Ganzhirn CT-Perfusion prinzipiell geeignet infratentorielle Infarkte darzustellen. Allerdings entgehen vor allem kleine Infarkte (< 19 mm) häufig dem Nachweis mittels CT-Perfusion.

II) Nach einem akuten Infarkt im Stromgebiet der Arteria cerebri media lässt sich in 35,3% der Fälle eine CCD beobachten. Dabei ist die Auftretenswahrscheinlichkeit der CCD mit der Infarktlokalisation (linke Hemisphäre und Frontallappen) sowie mit dem Ausmaß der Perfusionsminderung, nicht jedoch mit dem Infarktvolumen, assoziiert.

III) Das Ausmaß des Mismatches zwischen den CT-Perfusionssequenzen CBF und CBV als Maß für die Penumbra hängt nicht von der Zeit zwischen Symptombeginn und Bildgebung, sondern vom Grad der leptomeningealen Kollateralisierung ab.

Summary

The introduction of whole-brain CT perfusion offers the possibility of gaining insight into pathophysiological changes of cerebral circulatory disorders in the case of acute stroke. As part of the present doctoral thesis three studies were conducted to highlight the role of whole-brain CT perfusion in stroke diagnostics.

I) Given the recent extension of scan width in the Z-axis the posterior fossa can be subjected to routine diagnostic imaging. Hence infratentorial perfusion alterations can be visualized. In the first study the diagnostic certainty of whole-brain CT perfusion to detect infratentorial infarcts was assessed.

II) A reduction of blood flow and metabolism in the cerebellar hemisphere contralateral to the damaged supratentorial hemisphere is called CCD („crossed cerebellar diaschisis“). In the second study the frequency as well as characteristics of CCD after acute infarcts of the medial cerebral artery were investigated.

III) The objective of the third study was to determine factors that have an impact on the extension of the penumbra. In contrast to the infarct core the structurally intact penumbra can be preserved from the transitions into irreversibly damaged brain tissue by therapeutic intervention. Information about the patient-specific proportional composition of the infarcted region into penumbra and infarct core on the basis of whole-brain CT perfusion provide the chance of individual therapeutic decision making.

In summary the following key messages can be made:

I) Given a specificity of 93.3% and a sensitivity of 41.4% whole-brain CT perfusion is in principle suitable to visualize infratentorial infarcts. However, CT perfusion often fails to detect small infarcts (< 19 mm).

II) CCD can be observed in 35.3% of cases of acute infarct of the medial cerebral artery. The probability of its occurrence is associated with the infarct location (left hemisphere and frontal lobe) and the degree of perfusion reduction, but not with the infarct volume.

III) The mismatch between the CT perfusion maps CBF and CBV as a scale of penumbra does not depend on the time between symptom onset and imaging, but on the degree of leptomeningeal collateralisation.

IV Literaturverzeichnis

1. Ginter E, Simko V, Wsolova L. Fall of the iron curtain: Male life expectancy in slovakia, in the czech republic and in europe. *Central European journal of public health*. 2009;17:171-174
2. Murray CJ, Vos T, Lozano R, Naghavi M, Flaxman AD, Michaud C, et al. Disability-adjusted life years (dalys) for 291 diseases and injuries in 21 regions, 1990-2010: A systematic analysis for the global burden of disease study 2010. *Lancet*. 2012;380:2197-2223
3. Lozano R, Naghavi M, Foreman K, Lim S, Shibuya K, Aboyans V, et al. Global and regional mortality from 235 causes of death for 20 age groups in 1990 and 2010: A systematic analysis for the global burden of disease study 2010. *Lancet*. 2012;380:2095-2128
4. Kolominsky-Rabas PL, Heuschmann PU, Marschall D, Emmert M, Baltzer N, Neundorfer B, et al. Lifetime cost of ischemic stroke in germany: Results and national projections from a population-based stroke registry: The erlangen stroke project. *Stroke; a journal of cerebral circulation*. 2006;37:1179-1183
5. Saka O, McGuire A, Wolfe C. Cost of stroke in the united kingdom. *Age and ageing*. 2009;38:27-32
6. Heuschmann PU. Schlaganfallhäufigkeit und versorgung von schlaganfallpatienten in deutschland. *Aktuelle Neurologie*. 2010;37:333-340
7. Mozaffarian D, Benjamin EJ, Go AS, Arnett DK, Blaha MJ, Cushman M, et al. Heart disease and stroke statistics--2015 update: A report from the american heart association. *Circulation*. 2015;131:e29-322
8. Quast MJ, Huang NC, Hillman GR, Kent TA. The evolution of acute stroke recorded by multimodal magnetic resonance imaging. *Magnetic resonance imaging*. 1993;11:465-471
9. Kanekar SG, Zacharia T, Roller R. Imaging of stroke: Part 2, pathophysiology at the molecular and cellular levels and corresponding imaging changes. *AJR. American journal of roentgenology*. 2012;198:63-74
10. Astrup J, Siesjo BK, Symon L. Thresholds in cerebral ischemia - the ischemic penumbra. *Stroke; a journal of cerebral circulation*. 1981;12:723-725
11. Powers WJ, Derdeyn CP, Biller J, Coffey CS, Hoh BL, Jauch EC, et al. 2015 american heart association/american stroke association focused update of the 2013 guidelines for the early management of patients with acute ischemic stroke regarding endovascular treatment: A guideline for healthcare professionals from the american heart association/american stroke association. *Stroke; a journal of cerebral circulation*. 2015;46:3020-3035
12. Jones TH, Morawetz RB, Crowell RM, Marcoux FW, FitzGibbon SJ, DeGirolami U, et al. Thresholds of focal cerebral ischemia in awake monkeys. *Journal of neurosurgery*. 1981;54:773-782
13. Sobolewski P, Kozera G, Kazmierski R, Michalak S, Szczuchniak W, Nyka W. Efficacy of cerebral thrombolysis in an extended 'time window'. *Journal of clinical pharmacy and therapeutics*. 2015;40:472-476
14. Hacke W, Donnan G, Fieschi C, Kaste M, von Kummer R, Broderick JP, et al. Association of outcome with early stroke treatment: Pooled analysis of atlantis, ecass, and ninds rt-pa stroke trials. *Lancet*. 2004;363:768-774

15. Hacke W, Kaste M, Bluhmki E, Brozman M, Davalos A, Guidetti D, et al. Thrombolysis with alteplase 3 to 4.5 hours after acute ischemic stroke. *The New England journal of medicine*. 2008;359:1317-1329
16. Tissue plasminogen activator for acute ischemic stroke. The national institute of neurological disorders and stroke rt-pa stroke study group. *The New England journal of medicine*. 1995;333:1581-1587
17. Goldstein JN, Marrero M, Masrur S, Pervez M, Barrocas AM, Abdullah A, et al. Management of thrombolysis-associated symptomatic intracerebral hemorrhage. *Archives of neurology*. 2010;67:965-969
18. Henninger N, Fisher M. Extending the time window for endovascular and pharmacological reperfusion. *Translational stroke research*. 2016
19. Tsivgoulis G, Safouris A, Katsanos AH, Arthur AS, Alexandrov AV. Mechanical thrombectomy for emergent large vessel occlusion: A critical appraisal of recent randomized controlled clinical trials. *Brain and behavior*. 2016;6:e00418
20. Berkhemer OA, Fransen PS, Beumer D, van den Berg LA, Lingsma HF, Yoo AJ, et al. A randomized trial of intraarterial treatment for acute ischemic stroke. *The New England journal of medicine*. 2015;372:11-20
21. Goyal M, Menon BK, van Zwam WH, Dippel DW, Mitchell PJ, Demchuk AM, et al. Endovascular thrombectomy after large-vessel ischaemic stroke: A meta-analysis of individual patient data from five randomised trials. *Lancet*. 2016;387:1723-1731
22. American Heart Association. News.Heart.Org/aha-names-top-10-heart-stroke-research-advances-of-2016/. 2017
23. Serena J, Davalos A, Segura T, Mostacero E, Castillo J. Stroke on awakening: Looking for a more rational management. *Cerebrovascular diseases*. 2003;16:128-133
24. Koton S, Tanne D, Bornstein NM, Investigators N. Ischemic stroke on awakening: Patients' characteristics, outcomes and potential for reperfusion therapy. *Neuroepidemiology*. 2012;39:149-153
25. Emberson J, Lees KR, Lyden P, Blackwell L, Albers G, Bluhmki E, et al. Effect of treatment delay, age, and stroke severity on the effects of intravenous thrombolysis with alteplase for acute ischaemic stroke: A meta-analysis of individual patient data from randomised trials. *Lancet*. 2014;384:1929-1935
26. de Los Rios la Rosa F, Khoury J, Kissela BM, Flaherty ML, Alwell K, Moomaw CJ, et al. Eligibility for intravenous recombinant tissue-type plasminogen activator within a population: The effect of the european cooperative acute stroke study (ecass) iii trial. *Stroke; a journal of cerebral circulation*. 2012;43:1591-1595
27. Burton KR, Dhanoa D, Aviv RI, Moody AR, Kapral MK, Laupacis A. Perfusion ct for selecting patients with acute ischemic stroke for intravenous thrombolytic therapy. *Radiology*. 2015;274:103-114
28. Davis S, Donnan GA. Time is penumbra: Imaging, selection and outcome. The johann jacob wepfer award 2014. *Cerebrovascular diseases*. 2014;38:59-72
29. Allmendinger AM, Tang ER, Lui YW, Spektor V. Imaging of stroke: Part 1, perfusion ct--overview of imaging technique, interpretation pearls, and common pitfalls. *AJR. American journal of roentgenology*. 2012;198:52-62
30. Axel L. Cerebral blood flow determination by rapid-sequence computed tomography: Theoretical analysis. *Radiology*. 1980;137:679-686
31. Bohner G, Forschler A, Hamm B, Lehmann R, Klingebiel R. [quantitative perfusion imaging by multi-slice ct in stroke patients]. *RoFo : Fortschritte auf dem Gebiete der Rontgenstrahlen und der Nuklearmedizin*. 2003;175:806-813

32. Hamberg LM, Hunter GJ, Halpern EF, Hoop B, Gazelle GS, Wolf GL. Quantitative high-resolution measurement of cerebrovascular physiology with slip-ring ct. *AJNR. American journal of neuroradiology*. 1996;17:639-650
33. Zhu G, Michel P, Aghaebrahim A, Patrie JT, Xin W, Eskandari A, et al. Computed tomography workup of patients suspected of acute ischemic stroke: Perfusion computed tomography adds value compared with clinical evaluation, noncontrast computed tomography, and computed tomography angiogram in terms of predicting outcome. *Stroke; a journal of cerebral circulation*. 2013;44:1049-1055
34. Hoeffner EG, Case I, Jain R, Gujar SK, Shah GV, Deveikis JP, et al. Cerebral perfusion ct: Technique and clinical applications. *Radiology*. 2004;231:632-644
35. Konstas AA, Goldmakher GV, Lee TY, Lev MH. Theoretic basis and technical implementations of ct perfusion in acute ischemic stroke, part 1: Theoretic basis. *AJNR. American journal of neuroradiology*. 2009;30:662-668
36. Latchaw RE, Alberts MJ, Lev MH, Connors JJ, Harbaugh RE, Higashida RT, et al. Recommendations for imaging of acute ischemic stroke: A scientific statement from the american heart association. *Stroke; a journal of cerebral circulation*. 2009;40:3646-3678
37. Hopyan J, Ciarallo A, Dowlatshahi D, Howard P, John V, Yeung R, et al. Certainty of stroke diagnosis: Incremental benefit with ct perfusion over noncontrast ct and ct angiography. *Radiology*. 2010;255:142-153
38. Leiva-Salinas C, Provenzale JM, Wintermark M. Responses to the 10 most frequently asked questions about perfusion ct. *AJR. American journal of roentgenology*. 2011;196:53-60
39. Thierfelder KM, von Baumgarten L, Lochelt AC, Meinel FG, Armbruster M, Beyer SE, et al. Diagnostic accuracy of whole-brain computed tomographic perfusion imaging in small-volume infarctions. *Investigative radiology*. 2014;49:236-242
40. Wintermark M, Fischbein NJ, Smith WS, Ko NU, Quist M, Dillon WP. Accuracy of dynamic perfusion ct with deconvolution in detecting acute hemispheric stroke. *AJNR. American journal of neuroradiology*. 2005;26:104-112
41. Ringleb PA, Veltkamp R. Akuttherapie des ischämischen schlaganfalls-ergänzung 2015: Rekanalisierende therapie. *Leitlinien der Deutschen Gesellschaft für Neurologie*. 2015
42. Kim SE, Choi CW, Yoon BW, Chung JK, Roh JH, Lee MC, et al. Crossed-cerebellar diaschisis in cerebral infarction: Technetium-99m-hmpao spect and mri. *Journal of nuclear medicine : official publication, Society of Nuclear Medicine*. 1997;38:14-19
43. Thierfelder KM, von Baumgarten L, Baumann AB, Meinel FG, Helck AD, Opherck C, et al. Penumbra pattern assessment in acute stroke patients: Comparison of quantitative and non-quantitative methods in whole brain ct perfusion. *PloS one*. 2014;9:e105413
44. Thierfelder KM, Sommer WH, Baumann AB, Klotz E, Meinel FG, Strobl FF, et al. Whole-brain ct perfusion: Reliability and reproducibility of volumetric perfusion deficit assessment in patients with acute ischemic stroke. *Neuroradiology*. 2013;55:827-835
45. Morhard D, Wirth CD, Fesl G, Schmidt C, Reiser MF, Becker CR, et al. Advantages of extended brain perfusion computed tomography: 9.6 cm coverage with time resolved computed tomography-angiography in comparison to standard stroke-computed tomography. *Investigative radiology*. 2010;45:363-369

46. Biesbroek JM, Niesten JM, Dankbaar JW, Biessels GJ, Velthuis BK, Reitsma JB, et al. Diagnostic accuracy of ct perfusion imaging for detecting acute ischemic stroke: A systematic review and meta-analysis. *Cerebrovascular diseases*. 2013;35:493-501
47. Sabarudin A, Subramaniam C, Sun Z. Cerebral ct angiography and ct perfusion in acute stroke detection: A systematic review of diagnostic value. *Quantitative imaging in medicine and surgery*. 2014;4:282-290
48. Hana T, Iwama J, Yokosako S, Yoshimura C, Arai N, Kuroi Y, et al. Sensitivity of ct perfusion for the diagnosis of cerebral infarction. *The journal of medical investigation : JMI*. 2014;61:41-45
49. Fukuyama H, Kameyama M, Harada K, Fujimoto N, Kobayashi A, Taki W, et al. Thalamic tumours invading the brain stem produce crossed cerebellar diaschisis demonstrated by pet. *Journal of neurology, neurosurgery, and psychiatry*. 1986;49:524-528
50. Mewasingh LD, Christiaens F, Aeby A, Christophe C, Dan B. Crossed cerebellar diaschisis secondary to refractory frontal seizures in childhood. *Seizure*. 2002;11:489-493
51. Otte A, Roelcke U, von Ammon K, Hausmann O, Maguire RP, Missimer J, et al. Crossed cerebellar diaschisis and brain tumor biochemistry studied with positron emission tomography, [18f]fluorodeoxyglucose and [11c]methionine. *Journal of the neurological sciences*. 1998;156:73-77
52. Engelborghs S, Pickut BA, Marien P, Opsomer F, De Deyn PP. Crossed cerebellar diaschisis and hemiataxia after thalamic hemorrhage. *Journal of neurology*. 2000;247:476-477
53. Tien RD, Ashdown BC. Crossed cerebellar diaschisis and crossed cerebellar atrophy: Correlation of mr findings, clinical symptoms, and supratentorial diseases in 26 patients. *AJR. American journal of roentgenology*. 1992;158:1155-1159

V. Veröffentlichungen

V.1 Diagnostic accuracy of whole-brain CT perfusion in the detection of acute infratentorial infarctions

Christine Bollwein*, Annika Plate, Wieland H. Sommer, Kolja M. Thierfelder, Hendrik Janssen, Maximilian F. Reiser, Andreas Straube, Louisa von Baumgarten

Neuroradiology. 2016 Nov; 58(11):1077-1085

Impact factor 2016: 2,3

* geteilte Erstautorenschaft

Diagnostic accuracy of whole-brain CT perfusion in the detection of acute infratentorial infarctions

Christine Bollwein¹ · Annika Plate² · Wieland H. Sommer¹ · Kolja M. Thierfelder¹ · Hendrik Janssen³ · Maximilian F. Reiser¹ · Andreas Straube² · Louisa von Baumgarten²

Received: 14 June 2016 / Accepted: 17 August 2016 / Published online: 20 September 2016
© Springer-Verlag Berlin Heidelberg 2016

Abstract

Introduction Although the diagnostic performance of whole-brain computed tomographic perfusion (WB-CTP) in the detection of supratentorial infarctions is well established, its value in the detection of infratentorial strokes remains less well defined. We examined its diagnostic accuracy in the detection of infratentorial infarctions and compared it to nonenhanced computed tomography (NECT), aiming to identify factors influencing its detection rate.

Methods Out of a cohort of 1380 patients who underwent WB-CTP due to suspected stroke, we retrospectively included all patients with MRI-confirmed infratentorial strokes and compared it to control patients without infratentorial strokes. Two blinded readers evaluated NECT and four different CTP maps independently for the presence and location of infratentorial ischemic perfusion deficits.

Results The study was designed as a retrospective case-control study and included 280 patients (cases/controls = 1/3). WB-CTP revealed a greater diagnostic sensitivity than NECT (41.4 vs. 17.1 %, $P = 0.003$). The specificity, however, was comparable (93.3 vs. 95.0 %). Mean transit time (MTT) and time to drain (TTD) were the most sensitive (41.4 and

40.0 %) and cerebral blood volume (CBV) the most specific (99.5 %) perfusion maps. Infarctions detected using WB-CTP were significantly larger than those not detected (15.0 vs. 2.2 ml; $P = 0.0007$); infarct location, however, did not influence the detection rate.

Conclusion The detection of infratentorial infarctions can be improved by assessing WB-CTP as part of the multimodal stroke workup. However, it remains a diagnostic challenge, especially small volume infarctions in the brainstem are likely to be missed.

Keywords Infratentorial infarction · Whole-brain CT perfusion imaging · Ischemic stroke

Abbreviations

WB-CTP	Whole-brain computed tomographic perfusion
MTT	Mean transit time
TTD	Time to drain
CBV	Cerebral blood volume
CBF	Cerebral blood flow
NECT	Nonenhanced CT
CTA	CT angiography

CB and AP contributed equally to this work.

✉ Louisa von Baumgarten
Louisa.vonBaumgarten@med.uni-muenchen.de

¹ Institute for Clinical Radiology, Ludwig-Maximilians-University Hospital of Munich, Munich, Germany

² Department of Neurology, Ludwig-Maximilians-University Hospital of Munich, Grosshadern Campus, Marchioninistr. 15, 81377 Munich, Germany

³ Department of Neuroradiology, South Nuremberg Hospital, Nuremberg, Germany

Introduction

About 20–30 % of all ischemic strokes involve the posterior or vertebrobasilar territory [1]. Ischemic lesions in the anterior and posterior circulation can result in identical symptoms. Therefore, the diagnosis of a posterior circulation stroke on the basis of clinical symptoms remains challenging [2, 3]. In the posterior circulation, relatively small infarcts can account for profound neurological disorders due to the compact arrangement of afferent and efferent fiber pathways as well as

regions with survival functions and cranial nerve nuclei in the brainstem. Delayed or incorrect diagnosis may have devastating consequences, including potentially preventable death or severe disability, if acute treatment or secondary prevention is deferred [4]. A confident diagnosis of infratentorial infarction can often only be reached after brain imaging [2]. So far, MRI with diffusion-weighted imaging (DWI) is considered “gold standard” in the diagnosis of posterior ischemic stroke [5]. In many centers, however, CT is more readily available in the acute phase than MRI and could be helpful if MRI is contraindicated or unavailable. With the introduction of CT perfusion, the use of CT was extended due to its ability to depict brain perfusion alterations in acute stroke. Many studies emphasized the gain of diagnostic power as CTP proved to be more sensitive than nonenhanced CT (NECT) alone, especially in the diagnosis of small volume infarctions [6–8]. Furthermore, it has been shown to be an appropriate tool for the delineation of infarct core and salvageable penumbra [9–12]. Standard CTP scans so far covered the ganglionic and supraganglionic levels but did not routinely cover the entire infratentorial structures [13]. This restriction was solved by the introduction of the whole-brain CT perfusion (WB-CTP) which increased the scan range in the *z*-axis and thus enabled to examine cerebellar as well as the brain stem perfusion [14]. However, data on the diagnostic accuracy of WB-CTP in the detection of infratentorial stroke is scarce. Therefore, the aim of the current study was to investigate the diagnostic accuracy of WB-CTP for the detection of acute infratentorial infarcts.

Methods

Study population and patient selection

The study was designed as a retrospective single-center case-control study at a large university hospital. Our initial cohort consisted of 1380 consecutive patients admitted to our institution undergoing multiparametric CT including WB-CTP due to suspected stroke between April 2009 and March 2013.

We retrospectively included all patients with

1. Complete multimodal CT scan dataset including NECT, WB-CTP, and CT angiography
2. An acute ischemic infarction in the infratentorial vertebrobasilar territory as confirmed by follow-up MRI

We excluded patients with

1. Other pathologies of the vertebrobasilar territory (hemorrhage, former infarction, tumor, hypoplasia of the vertebral artery)

2. CTP with nondiagnostic quality and/or insufficient cerebellar coverage

CTP parameters were analyzed by unbiased readers who were blinded to clinical history, CT angiography, and NECT. Therefore, we restricted our study cohort to patients with acute infratentorial infarction and excluded patients with former infarction, tumor, hemorrhage (and potential associated vasospasm), as well as patients with hypoplastic vertebral arteries. All of these conditions can potentially mimic perfusion alterations suggestive of ischemia [15, 16]; however, they can easily be ruled out in clinical routine by assessing multimodal CT datasets including NECT and CT angiography.

Out of all patients who received multiparametric CT due to suspected stroke, we selected control patients who fulfilled the same inclusion and exclusion criteria as our case cohort but did not show an acute infratentorial ischemia on follow-up MRI. We used a ratio of cases to controls of 1:3 in order to prevent a biased reading [17–19]. Furthermore, a prevalence of 25 % represents the frequency of vertebrobasilar infarcts among stroke patients [1]. The institutional review board approved the study and waived requirement for informed consent.

CT examination protocol

The multiparametric CT protocol consisted of NECT to exclude intracranial hemorrhage, a supraaortic CT angiography (CTA), and WB-CTP, all performed using one of the following CT scanners: SOMATOM Definition AS+, a 128-slice CT scanner; SOMATOM Definition Flash, a 128-slice dual source CT scanner; and SOMATOM Definition Edge, a 128-slice CT scanner (all by Siemens Healthcare, Erlangen, Germany).

WB-CTP images were obtained with 0.6-mm collimation and scan coverage of 100 mm in the *z*-axis acquired by a toggling table technique. One scan was acquired every 1.5 s with the following imaging parameters: tube voltage 80 kV, tube current 200 mAs, and computed tomography dose index (CTDI_{vol}) 276.21 mGy. Thirty-five milliliters of highly iodinated contrast agent were administered intravenously at a flow rate of 5 ml/s, followed by a saline flush of 40 ml at 5 ml/s. Thirty-one axial slices with a thickness of 10 mm and increment of 3 mm were reconstructed from the dataset.

CT perfusion image processing

The processing of source images was performed with the SYNGO Volume Perfusion CT Neuro software using a semiautomated deconvolution algorithm (Auto Stroke MTT). Datasets were transferred to a dedicated workstation (Syngo MMWP, VA 21A; Siemens Healthcare, Erlangen, Germany). Parametric maps were created by selecting the arterial input function from a main arterial vessel and the venous output

function from the superior sagittal sinus. A series of 31 color-coded images was generated for each of the hemodynamic parameters cerebral blood flow (CBF), cerebral blood volume (CBV), mean transit time (MTT), and time to drain (TTD). The color images were saved in DICOM format and displayed on default window settings for further evaluation.

MRI follow-up

The MRI follow-up study comprised a T2* sequence, a fluid-attenuated inversion recovery (FLAIR) sequence, a DWI sequence, and a time-of-flight (TOF)-MR angiography. The volume of the final infarction was measured in the DWI sequence with a b-value of 1000.

Image analysis

The CT perfusion images were studied independently by two readers who were blinded to NECT, CTA, and follow-up MRI, as well as clinical data (one neurologist (*BLINDED*) with 9 years and one neurologist (*BLINDED*) with 6 years of experience in multiparametric CT reading). In case of disagreement, a consensus was reached in a separate session.

The CTP parameter datasets were presented one after the other. The reader assessed the presence and location of an infratentorial perfusion deficit for each of the perfusion maps. Patients were classified to have an acute ischemia on WB-CTP if significant perfusion alterations were present in at least two perfusion parameter maps in the same location. NECT images were randomly presented to the readers in a separate session several weeks after the CTP reading. In case of disagreement, a consensus was reached in a separate session.

The final infarction volume was quantified based on the DWI sequence of the follow-up MR as previously described, using the software OsiriX V.4.0 on a 27-in. iMac computer (Apple Inc., Cupertino, CA, USA) [6]. Briefly, infarct volume was calculated by delineating regions of interest around the lesions on the diffusion-weighted images. The volume was calculated in milliliters by multiplying the lesion area by the slice thickness. The final infarct diameter was measured on the slice showing the maximal infarct extent.

Statistical analysis

All statistical analyses were performed using Excel (Microsoft® Excel® 2013) and MedCalc (MedCalc Software© 1993–2014). On the basis of the two independent readings, the level of interrater agreement in the evaluation of perfusion maps was assessed by calculation of the kappa coefficient. Sensitivity and specificity were determined according to the consensus reading for each of the perfusion parameters and the NECT images. The differences between the

infratentorial infarctions classified as CTP positive and CTP negative were investigated using the Mann-Whitney *U* test in case of nonnormal distribution and the chi-squared test in case of values that were expressed as rates or proportions. To test for normal distribution, the Shapiro-Wilk test was applied to the continuous data. Finally, a subanalysis was conducted to evaluate the sensitivity of CT perfusion and NECT in the detection of different types of infratentorial infarctions. The significance level for all tests was set at $P < 0.05$. Data are expressed as median \pm interquartile range or mean \pm standard deviation/95 % confidence interval as appropriate.

Results

Patient cohort

Between April 2009 and March 2013, a total of 1380 patients underwent initial multimodal cranial CT due to suspected stroke. Among these, 84 had an acute infratentorial ischemic stroke as confirmed by MRI and were included for further analysis. Of these, 14 patients were excluded either due to another pathology of the vertebrobasilar territory ($N = 5$), insufficient infratentorial coverage ($N = 6$), or technical problems of data acquisition (poor bolus timing, $N = 3$). The remaining 70 patients formed our patient sample and were compared to the control group. Procedure of patient selection is illustrated in Fig. 1.

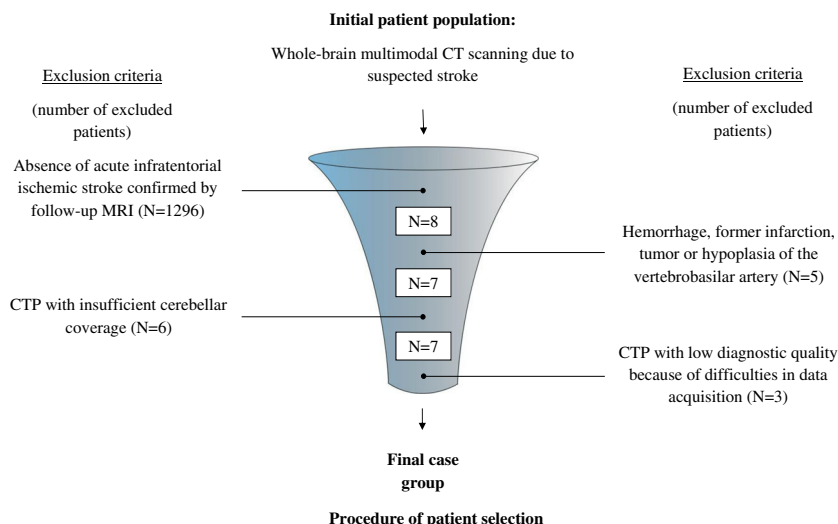
As shown in Table 1, there were no significant differences with respect to age, sex, time from symptom onset, time between CTP and follow-up MRI, the presence of supratentorial infarction, or thrombolytic therapy between the case and control group. The only statistical significant difference was detected in the rate of mechanical recanalization (17.1 % for patients with infarctions of the posterior circulation vs. 6.7 % for control patients with supratentorial strokes, $P = 0.0174$). The final infratentorial infarction volume averaged 7.5 ± 22.6 ml, and the mean final diameter was 24 ± 21 mm.

Overall diagnostic accuracy of WB-CTP

Of the 70 patients with confirmed infratentorial infarctions, 29 showed significant perfusion alterations in at least two perfusion parameter maps, resulting in an overall sensitivity of 41.4 % (confidence interval (CI) 29.8–53.8 %). Within the control group of 210 patients, 14 individuals were considered to have significant perfusion alterations, resulting in an overall specificity of 93.3 % (CI 89.1–96.3 %).

The data on diagnostic accuracy of WB-CTP is shown in Table 2, and representative patient examples are highlighted in Fig. 2a and b.

Fig. 1 Procedure of patient selection



The different parameter maps ranged considerably with respect to the detection of infratentorial infarcts: sensitivity ranged from 8.6 to 41.4 % and specificity from 93.3 to 99.5 %. MTT (41.4 %) and TTD (40.0 %) turned out to be the most sensitive parameter maps, whereas CBV (99.5 %) was the most specific (Table 3).

Identification of factors influencing diagnostic accuracy

To elucidate which factors influence the detection rate of infratentorial ischemic lesions on WB-CTP, we compared patients whose infarcts had been detected with patients

whose infarcts had remained indiscernible in initial WB-CTP imaging. Analysis revealed that infarctions that were correctly identified had a significantly larger mean infarct volume (15.0 ml for CTP positive vs. 2.2 ml for CTP negative, $P = 0.0007$) as well as a significantly larger mean infarct diameter (33 mm for CTP positive vs. 18 mm for CTP negative, $P = 0.0005$). No other significant association was observed between the other parameters analyzed (percentage of supratentorial infarction, time from symptom onset, time between CT and follow-up imaging, rtPA, mechanical recanalization, age, and gender) and the detection rate of infratentorial infarctions (see Table 4).

Table 1 Characteristics of the study population ($N = 210$)

	Patient group		Control group		P value
	Value	Range	Value	Range	
<i>N</i>	70		210		
Age (years) [IR]	72.5 [59.0;77.0]	31–94	69.0 [57.0;78.0]	27–97	0.4403 ^b
Male gender (%)	53.8	–	65.7	–	0.1092 ^c
Time from symptom onset (min) [IR] ^a	143.0 [102.0;299.75]	12–1268	129.5 [92.5;188.5]	16–1141	0.2732 ^b
Time between CTP and FU-MRI (h) [IR]	34.3 [18.2;66.1]	0.3–766.4	37.1 [19.8;72.4]	1–811.6	0.6406 ^b
Supratentorial infarction (%)	45.7	–	55.2	–	0.2134 ^c
Thrombolytic therapy (%)	31.4	–	23.8	–	0.0659 ^c
Mechanical recanalization (%)	17.1	–	6.7	–	0.0174 ^{*c}
Final infarct volume (ml) [IR]	8.6 [1.9;31.2]	0.1–133.9	–	–	–
Final infarct diameter (mm) [IR]	19.1 [9.6;28.4]	3–107	–	–	–

IR interquartile range

*Statistically significant

^a Available for 50.4 % of subjects

^b Mann-Whitney test

^c Chi-squared test

Table 2 Proportion of CTP (+) and CTP (–) cases within the patient and the control group

	CTP (+)	CTP (–)	<i>P</i> value
Patient group (<i>N</i> = 70)	29 (41.4 %) ^a	41 (58.6 %) ^b	<0.0001*
Control group (<i>N</i> = 210)	14 (6.7 %) ^a	196 (93.3 %) ^b	

*Statistically significant (chi-squared test)

^a Sensitivity^b Specificity**Detection rate: role of infarct location and infarct size**

Finally, the detection rates of infratentorial infarctions were compared with respect to their location (cerebellum, brain stem) and size. During WB-CTP reading, cerebellar infarctions tended to be detected more reliably than brain stem infarctions (sensitivity 58.2 and 28.1 %, respectively), although the difference failed to reach statistical significance ($P = 0.06$). To assess the detection rates with respect to the size of infratentorial infarctions, we analyzed the detection rates of small-volume infarctions (Table 5). Because of a lack of unequivocal definitions of lacunar or small-volume infarcts in the literature, we determined the median diameter of all infratentorial infarctions in our patient cohort, which was 19 mm. This diameter was set as an arbitrary threshold to distinguish small (≤ 19 mm) and larger infarcts (>19 mm). In general, sensitivity for infratentorial infarctions was significantly higher for infarcts >19 mm than for infarctions ≤ 19 mm. This proved to be valid for infarcts located in the cerebellum (68.0 % for cerebellum >19 mm vs. 23.1 % for cerebellum ≤ 19 mm, $P = 0.0070$), whereas infarcts in the brain stem were equally likely to be detected regardless of a diameter beyond or below 19 mm. Additionally, by comparing the

Table 3 Diagnostic accuracy of different CTP parameters in the detection of infratentorial

	Sensitivity [95 % CI]	Specificity [95 % CI]
Overall	41.4 [29.8;53.8]	93.3 [89.1;96.3]
CBF	38.6 [27.2;60.0]	93.8 [89.7;96.7]
CBV	8.6 [3.2;17.7]	99.5 [97.4;99.9]
MTT	41.4 [29.8;53.8]	93.3 [89.1;96.3]
TTD	40.0 [28.5;52.4]	93.8 [89.7;96.7]

CBF cerebral blood flow, CBV cerebral blood volume, MTT mean transit time, TTD time to drain

sensitivity of CTP in detecting small and large infarctions, we found out that there is no significant difference between the detection rates of infarctions located in the cerebellum and in the brainstem (≤ 19 mm: 23.1 vs. 22.7 %, $P = 0.6945$, and >19 mm: 68.0 vs. 40.0 %, $P = 0.2519$).

Detection rates of WB-CTP compared to NECT

NECT correctly identified 12 out of 70 patients with infratentorial strokes (Table 6). The resulting sensitivity of 17.14 % (CI 9.18–28.03 %) is significantly lower than the sensitivity of WB-CTP (41.4 %, CI 29.8–53.8 %, $P = 0.0030$). The specificity of NECT is 95.0 % (CI 89.97–97.97 %), which is comparable to the sensitivity of WB-CTP (93.3 %, CI 89.1–96.3 %). Table 6 indicates the sensitivity of NECT compared to WB-CTP for cerebellar and brain stem infarctions as well as for small (≤ 19 mm) and large (>19 mm) infarctions. Notably, NECT failed to detect small infarctions (sensitivity 0 %), whereas these could be detected by WB-CTP in 22.9 % (CI 9.9–45.0, $P = 0.0085$).

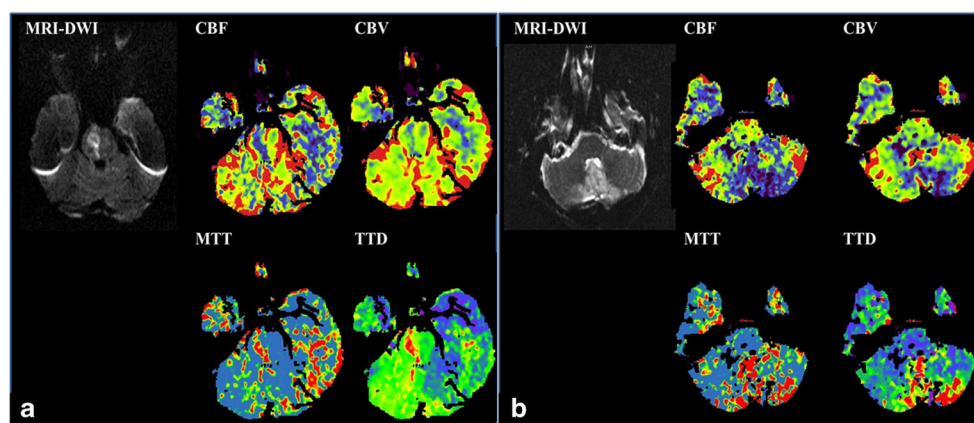


Fig. 2 a Ninety-two-year-old female presenting with dysarthria, dysphagia, and a left-sided hemiparesis. CTP was performed 90 min after symptom onset and showed a right-sided paramedian hypoperfusion of the pons with a mismatch between CBF and CBV. CTA revealed a thrombotic occlusion of the basilar artery. The patient received iv-thrombolysis immediately after multimodal CT imaging. The ischemic lesion on follow-up MRI reveals a right paramedian pons

infarction. **b** Fifty-two-year-old male with a left-sided occlusion of the vertebral artery caused by dissection leading to nystagmus, singultus, left-sided ptosis and facial paresis. CTP showed a mismatch in the caudal parts of the left cerebellar hemisphere. Neither systemic lysis nor mechanical recanalization was performed because of unknown symptom onset. The follow-up MRI shows a left-sided PICA infarct

Table 4 Comparison between CTP (+) and CTP (–) infratentorial infarctions

	CTP (+) (N = 29)	CTP (–) (N = 41)	P value
Volume of infratentorial infarction (ml) [IR]	24.4 [8.6;54.5]	4.7 [1.2;16.3]	0.0007 ^{*a}
Diameter of infratentorial infarction (mm) [IR]	26.3 [18.0;39.0]	13.6 [8.7;21.8]	0.0005 ^{*a}
Supratentorial infarction (%)	34.5	53.7	0.1793 ^b
Time between CT and follow-up MRI (h) [IR]	29.2 [12.2;47.9]	44.4 [20.4;83.6]	0.1285 ^a
Thrombolytic therapy (%)	31.0	31.7	0.8402 ^b
Mechanical recanalization (%)	17.2	17.1	0.7615 ^b
Age (years) [IR]	73.0 [65.5;78.8]	72.0 [55.8;76.0]	0.2673 ^a
Male gender (%)	62.1	68.3	0.7758 ^b

IR interquartile range

*Statistically significant

^a Mann-Whitney test

^b Chi-squared test

Furthermore, WB-CTP proved to be superior in the detection rate of cerebellar infarctions (NECT 18.42 %, CI 7.41;37.95 vs. WB-CTP 52.6, CI 32.2;81.3, $P = 0.0040$).

Discussion

WB-CTP has a sensitivity of 41.4 % and a specificity of 93.3 % in the detection of infratentorial infarcts. MTT and TTD were most sensitive, whereas CBV proved to be particularly specific in confirming ischemic lesions. The detection rate of WB-CTP increases with infarct volume and infarct diameter. Compared to NECT, which reaches an overall diagnostic sensitivity of 17.1 %, WB-CTP is significantly more sensitive in the detection of infratentorial infarctions, in particular of small infarctions which are often not detected by NECT alone.

Despite the considerable specificity, the overall sensitivity of WB-CTP in the detection of infratentorial stroke merely averaged 41.4 %. This result can most probably be attributed to the high proportion of small infarcts that constituted the vast majority in our patient group. The major drawback of CTP to

depict lacunar or small volume infarcts was already highlighted by a number of other CTP studies [20–25]. It was shown that CTP detected 62 % of all MRI-DWI-confirmed lacunar infarcts; however, CTP was more sensitive in the detection of supratentorial than of infratentorial strokes. Similar to our results, NECT only yielded an overall sensitivity of 19 % [25]. Lee et al. report a sensitivity of CTP of about 81.4 % and a specificity of 96.0 % in the detection of 32 patients with infratentorial infarcts [26]. In contrast to our study, the authors excluded lacunar infarctions from their analysis, which could explain the comparatively higher sensitivity of this study. Importantly, no information on the relation of detection rate and infarction volume was given by the authors. Furthermore, in this study, the duration from time from symptom onset to imaging (540 vs. 231 min) was much longer, potentially resulting in more sustained ischemic changes [26]. Another study investigating the diagnostic value of CTP in posterior circulation infarcts revealed an overall sensitivity of 74 %—ranging from 85 % for ischemic lesions in the PCA territory and 10 % in pons and midbrain [27]. An overall sensitivity of about 41 % in the detection of infratentorial infarcts in an unselected patient cohort with confirmed posterior circulation

Table 5 Sensitivity of WB-CTP in different types of infratentorial infarcts

	N	No. detected	Sensitivity [95 % CI]	P value
Overall	70	29	41.4 [29.8;53.8]	–
Cerebellum	38	20	52.6 [32.2;81.3]	0.0673 ^a
Brain stem	32	9	28.1 [12.9;53.4]	
≤19 mm	35	8	22.9 [9.9;45.0]	0.0115 ^{*a}
>19 mm	35	21	60.0 [37.1;91.7]	
Cerebellum ≤19 mm	13	3	23.1 [4.8;67.4]	0.0070 ^{*a}
Cerebellum >19 mm	25	17	68.0 [39.6;100.0]	
Brain stem ≤19 mm	22	5	22.7 [7.4;53.0]	0.5586 ^a
Brain stem >19 mm	10	4	40.0 [10.9;100.0]	

CI confidence interval

*Statistically significant

^a Chi-squared test

Table 6 Sensitivity of NECT and WB-CTP in the detection of infratentorial infarctions

	N	NECT		WB-CTP		P value
		No. detected	Sensitivity [95 % CI]	No. detected	Sensitivity [95 % CI]	
Overall	70	12	17.14 [9.18;28.03]	29	41.4 [29.8;53.8]	0.0030* ^a
Cerebellum	38	7	18.42 [7.41;37.95]	20	52.6 [32.2;81.3]	0.0040* ^a
Brain stem	32	5	15.63 [5.07;36.46]	9	28.1 [12.9;53.4]	0.3643 ^a
≤19 mm	35	0	0	8	22.9 [9.9;45.0]	0.0085* ^a
>19 mm	35	12	34.29 [17.72;59.89]	21	60.0 [37.1;91.7]	0.0554 ^a

CI confidence interval

*Statistically significant

^a Chi-squared test

infarction including all sizes of infarcts seems to represent the diagnostic sensitivity of WB-CTP in daily routine adequately.

Cerebellar infarcts tended to be more likely detected than brain stem infarcts. However, this can be attributed to the fact that strokes in the cerebellum are usually larger than those in the brain stem. We failed to provide evidence for a significant influence of the infarct location on the detection rate of CTP for infratentorial strokes. With respect to the single perfusion parameters, MTT and TTD were the most sensitive maps identifying infratentorial infarctions, whereas CBV showed a higher specificity. Perfusion disturbances in the posterior circulation have previously been reported to be the most frequent and most pronounced on MTT parameter maps [28].

Preceding studies investigating the specificity of CTP in the detection of supratentorial infarcts reported a wide range of values (61–100 %) [29, 20, 30, 24]. We can demonstrate that infratentorial infarctions can be detected with a reasonable specificity of 93.3 % despite potential shortcomings related to beam hardening artifacts and different arterial supplying system in the posterior fossa [29].

MRI with diffusion-weighted imaging is still considered as the modality of choice for suspected stroke. However, it is often unavailable in the emergency setting, is more time consuming, and cannot be performed in patients with metallic foreign bodies or incompatible pacemakers. MRI is more sensitive than NECT in the diagnosis of an acute stroke in an unselected patient cohort (all vascular territories included), indicating an 83 % sensitivity in the first 24 h when DWI MRI is performed (vs. 26 % sensitivity using NECT) [31, 32]. In selected patient cohorts, NECT provides a reliable mean of identifying medium-to-large areas of acute ischemic changes. Abnormalities of NECT have been reported in 40–50 % of all acute hemispheric ischemic strokes [33, 34]. However, acute ischemic changes are often subtle and there is a great interobserver and intraobserver variability [35]. Small volume infarcts in the early stages of stroke can be significantly more difficult to detect [36]. Consistent with our results, the overall sensitivity of NECT in the detection of posterior infarctions

(including the PCA territory) has been reported to be 31 %, for pons and midbrain infarctions; however, it was reported to be 10 % only [27]. Our data demonstrates that WB-CTP is more sensitive in the detection of infratentorial infarctions than NECT. In particular, small infarctions are likely to be missed on NECT but can be detected using WB-CTP, indicating the additional diagnostic value of CTP imaging in this setting.

Given the retrospective study design, our data suffer from some inevitable limitations. We were not able to control the time between CTP and follow-up MRI. Intravenous thrombolytic therapy may have influenced sensitivity and specificity because it can lead to reperfusion in the potentially salvageable penumbra. Consequently, ischemic but still viable regions may not progress to infarction in treated patients, leading to false-positive findings. Similarly, diffusion-weighted imaging can seldom be negative for clinically definite posterior circulation infarcts, particularly brainstem infarcts [32, 3]. Furthermore, CTP images were just visually assessed without the use of quantitative tools. This approach, however, commonly reflects the methodology of radiologic reporting of CTP maps [6]. Moreover, we excluded patients with former infarction, hemorrhage, or tumor in the vertebrobasilar territory and hyoplastic vertebral artery from the study for the reasons given above. This could have led to a distortion of the results, particularly to a reduction of the number of false-positive cases and thus to an overestimation of specificity.

In conclusion, WB-CTP can detect infratentorial infarctions in an unselected stroke-patient cohort with a sensitivity of 41 %. As the majority of infarctions in the infratentorial location consist of comparatively small infarctions, the low sensitivity reflects the well-known drawback of CTP in the detection of small-volume infarctions. However, the sensitivity increases with infarct size and is superior to that of NECT alone. Furthermore, it potentially allows for the detection of a salvageable penumbra. Overall, the confident diagnosis of infratentorial infarctions remains a diagnostic challenge, especially small-volume infarctions are likely to be missed.

Compliance with ethical standards We declare that all human studies have been approved by the institutional ethics committee of the Medical Faculty of the Ludwig-Maximilians University Munich and have therefore been performed in accordance with the ethical standards laid down in the 1964 Declaration of Helsinki and its later amendments. We declare that the ethics committee waived informed patient consent.

Conflict of interest We declare that we have no conflict of interest.

References

- Bogousslavsky J, Van Melle G, Regli F (1988) The Lausanne Stroke Registry: analysis of 1,000 consecutive patients with first stroke. *Stroke* 19(9):1083–1092
- Flossmann E, Redgrave JN, Briley D, Rothwell PM (2008) Reliability of clinical diagnosis of the symptomatic vascular territory in patients with recent transient ischemic attack or minor stroke. *Stroke* 39(9):2457–2460. doi:10.1161/STROKEAHA.107.511428
- Tao WD, Liu M, Fisher M, Wang DR, Li J, Furie KL, Hao ZL, Lin S, Zhang CF, Zeng QT, Wu B (2012) Posterior versus anterior circulation infarction: how different are the neurological deficits? *Stroke* 43(8):2060–2065. doi:10.1161/STROKEAHA.112.652420
- Kuruvilla A, Bhattacharya P, Rajamani K, Chaturvedi S (2011) Factors associated with misdiagnosis of acute stroke in young adults. *J Stroke Cerebrovasc Dis* 20(6):523–527. doi:10.1016/j.jstrokecerebrovasdis.2010.03.005
- Muir KW, Buchan A, von Kummer R, Rother J, Baron JC (2006) Imaging of acute stroke. *Lancet Neurol* 5(9):755–768. doi:10.1016/S1474-4422(06)70545-2
- Thierfelder KM, Sommer WH, Baumann AB, Klotz E, Meinel FG, Strobl FF, Nikolaou K, Reiser MF, von Baumgarten L (2013) Whole-brain CT perfusion: reliability and reproducibility of volumetric perfusion deficit assessment in patients with acute ischemic stroke. *Neuroradiology* 55(7):827–835. doi:10.1007/s00234-013-1179-0
- Lin K, Do KG, Ong P, Shapiro M, Babb JS, Siller KA, Pramanik BK (2009) Perfusion CT improves diagnostic accuracy for hyperacute ischemic stroke in the 3-hour window: study of 100 patients with diffusion MRI confirmation. *Cerebrovasc Dis* 28(1):72–79. doi:10.1159/000219300
- Bivard A, Spratt N, Levi C, Parsons M (2011) Perfusion computer tomography: imaging and clinical validation in acute ischaemic stroke. *Brain* 134(Pt 11):3408–3416. doi:10.1093/brain/awr257
- Wintermark M, Flanders AE, Velthuis B, Meuli R, van Leeuwen M, Goldsher D, Pineda C, Serena J, van der Schaaf I, Waaijer A, Anderson J, Nesbit G, Gabriely I, Medina V, Quiles A, Pohlman S, Quist M, Schnyder P, Bogousslavsky J, Dillon WP, Pedraza S (2006) Perfusion-CT assessment of infarct core and penumbra: receiver operating characteristic curve analysis in 130 patients suspected of acute hemispheric stroke. *Stroke* 37(4):979–985. doi:10.1161/01.STR.0000209238.61459.39
- Nabavi DG, Cenic A, Henderson S, Gelb AW, Lee TY (2001) Perfusion mapping using computed tomography allows accurate prediction of cerebral infarction in experimental brain ischemia. *Stroke* 32(1):175–183
- Wintermark M, Reichhart M, Cuisenaire O, Maeder P, Thiran JP, Schnyder P, Bogousslavsky J, Meuli R (2002) Comparison of admission perfusion computed tomography and qualitative diffusion- and perfusion-weighted magnetic resonance imaging in acute stroke patients. *Stroke* 33(8):2025–2031
- Schaefer PW, Barak ER, Kamalian S, Gharai LR, Schwamm L, Gonzalez RG, Lev MH (2008) Quantitative assessment of core/penumbra mismatch in acute stroke: CT and MR perfusion imaging are strongly correlated when sufficient brain volume is imaged. *Stroke* 39(11):2986–2992. doi:10.1161/STROKEAHA.107.513358
- Parsons MW (2008) Perfusion CT: is it clinically useful? *Int J Stroke* 3(1):41–50. doi:10.1111/j.1747-4949.2008.00175.x
- Morhard D, Wirth CD, Fesl G, Schmidt C, Reiser MF, Becker CR, Ertl-Wagner B (2010) Advantages of extended brain perfusion computed tomography: 9.6 cm coverage with time resolved computed tomography-angiography in comparison to standard stroke-computed tomography. *Investig Radiol* 45(7):363–369. doi:10.1097/RLL.0b013e3181e1956f
- Best AC, Acosta NR, Fraser JE, Borges MT, Brega KE, Anderson T, Neumann RT, Ree A, Bert RJ (2012) Recognizing false ischemic penumbras in CT brain perfusion studies. *Radiographics* 32(4):1179–1196. doi:10.1148/rg.324105742
- Thierfelder KM, Baumann AB, Sommer WH, Armbruster M, Opherck C, Janssen H, Reiser MF, Straube A, von Baumgarten L (2014) Vertebral artery hypoplasia: frequency and effect on cerebellar blood flow characteristics. *Stroke* 45(5):1363–1368. doi:10.1161/STROKEAHA.113.004188
- Rothman KJ (2012) *Epidemiology: an introduction*, second edn. Oxford University Press, New York; Oxford
- Ury HK (1975) Efficiency of case-control studies with multiple controls per case: continuous or dichotomous data. *Biometrics* 31(3):643–649
- Miettinen OS (1969) Individual matching with multiple controls in the case of all-or-none responses. *Biometrics* 25(2):339–355
- Biesbroek JM, Niesten JM, Dankbaar JW, Biessels GJ, Velthuis BK, Reitsma JB, van der Schaaf IC (2013) Diagnostic accuracy of CT perfusion imaging for detecting acute ischemic stroke: a systematic review and meta-analysis. *Cerebrovasc Dis* 35(6):493–501. doi:10.1159/000350200
- Hana T, Iwama J, Yokosako S, Yoshimura C, Arai N, Kuroi Y, Koseki H, Akiyama M, Hirota K, Ohbuchi H, Hagiwara S, Tani S, Sasahara A, Kasuya H (2014) Sensitivity of CT perfusion for the diagnosis of cerebral infarction. *J Med Investig* 61(1–2):41–45
- Campbell BC, Weir L, Desmond PM, Tu HT, Hand PJ, Yan B, Donnagan GA, Parsons MW, Davis SM (2013) CT perfusion improves diagnostic accuracy and confidence in acute ischaemic stroke. *J Neurol Neurosurg Psychiatry* 84(6):613–618. doi:10.1136/jnnp-2012-303752
- Lin K, Do KG, Ong P, Shapiro M, Babb JS, Siller KA, Pramanik BK (2009) Perfusion CT improves diagnostic accuracy for hyperacute ischemic stroke in the 3-h window: study of 100 patients with diffusion MRI confirmation. *Cerebrovasc Dis* 28(1):72–79. doi:10.1159/000219300
- Thierfelder KM, von Baumgarten L, Lochelt AC, Meinel FG, Armbruster M, Beyer SE, Patzig M, Opherck C, Reiser MF, Sommer WH (2014) Diagnostic accuracy of whole-brain computed tomographic perfusion imaging in small-volume infarctions. *Investig Radiol* 49(4):236–242. doi:10.1097/RLL.0000000000000023
- Rudilosso S, Urra X, San Roman L, Laredo C, Lopez-Rueda A, Amaro S, Oleaga L, Chamorro A (2015) Perfusion deficits and mismatch in patients with acute lacunar infarcts studied with whole-brain CT perfusion. *AJNR Am J Neuroradiol* 36(8):1407–1412. doi:10.3174/ajnr.A4303
- Lee IH, You JH, Lee JY, Whang K, Kim MS, Kim YJ, Lee MS, Brain Research G (2010) Accuracy of the detection of infratentorial stroke lesions using perfusion CT: an experimenter-blinded study. *Neuroradiology* 52(12):1095–1100. doi:10.1007/s00234-010-0689-2

27. van der Hoeven EJ, Dankbaar JW, Algra A, Vos JA, Niesten JM, van Seeters T, van der Schaaf IC, Schonewille WJ, Kappelle LJ, Velthuis BK, Investigators D (2015) Additional diagnostic value of computed tomography perfusion for detection of acute ischemic stroke in the posterior circulation. *Stroke* 46(4):1113–1115. doi:10.1161/STROKEAHA.115.008718
28. Pallesen LP, Gerber J, Dzialowski I, van der Hoeven EJ, Michel P, Pfefferkorn T, Ozdoba C, Kappelle LJ, Wiedemann B, Khomenko A, Algra A, Hill MD, von Kummer R, Demchuk AM, Schonewille WJ, Puetz V (2015) Diagnostic and prognostic impact of pc-ASPECTS applied to perfusion CT in the basilar artery international cooperation study. *Journal of neuroimaging : official journal of the American Society of Neuroimaging* 25(3):384–389. doi:10.1111/jon.12130
29. Wintermark M, Fischbein NJ, Smith WS, Ko NU, Quist M, Dillon WP (2005) Accuracy of dynamic perfusion CT with deconvolution in detecting acute hemispheric stroke. *AJNR Am J Neuroradiol* 26(1):104–112
30. Sabarudin A, Subramaniam C, Sun Z (2014) Cerebral CT angiography and CT perfusion in acute stroke detection: a systematic review of diagnostic value. *Quantitative imaging in medicine and surgery* 4(4):282–290. doi:10.3978/j.issn.2223-4292.2014.07.10
31. Chalela JA, Kidwell CS, Nentwich LM, Luby M, Butman JA, Demchuk AM, Hill MD, Patronas N, Latour L, Warach S (2007) Magnetic resonance imaging and computed tomography in emergency assessment of patients with suspected acute stroke: a prospective comparison. *Lancet* 369(9558):293–298. doi:10.1016/S0140-6736(07)60151-2
32. Edlow JA, Newman-Toker DE, Savitz SI (2008) Diagnosis and initial management of cerebellar infarction. *Lancet Neurol* 7(10):951–964. doi:10.1016/S1474-4422(08)70216-3
33. von Kummer R, Bourquain H, Bastianello S, Bozzao L, Manelfe C, Meier D, Hacke W (2001) Early prediction of irreversible brain damage after ischemic stroke at CT. *Radiology* 219(1):95–100. doi:10.1148/radiology.219.1.r01ap0695
34. von Kummer R, Nolte PN, Schnittger H, Thron A, Ringelstein EB (1996) Detectability of cerebral hemisphere ischaemic infarcts by CT within 6 h of stroke. *Neuroradiology* 38(1):31–33
35. Grotta JC, Chiu D, Lu M, Patel S, Levine SR, Tilley BC, Brott TG, Haley EC Jr, Lyden PD, Kothari R, Frankel M, Lewandowski CA, Libman R, Kwiatkowski T, Broderick JP, Marler JR, Corrigan J, Huff S, Mitsias P, Talati S, Tanne D (1999) Agreement and variability in the interpretation of early CT changes in stroke patients qualifying for intravenous rtPA therapy. *Stroke* 30(8):1528–1533
36. Wardlaw JM, Farrall AJ, Perry D, von Kummer R, Mielke O, Moulin T, Ciccone A, Hill M (2007) Factors influencing the detection of early CT signs of cerebral ischemia: an internet-based, international multiobserver study. *Stroke* 38(4):1250–1256. doi:10.1161/01.STR.0000259715.53166.25

V.2 Crossed cerebellar diaschisis in patients with acute middle cerebral artery infarction: Occurrence and perfusion characteristics

Wieland H. Sommer, **Christine Bollwein***, Kolja M. Thierfelder, Alena Baumann, Hendrik Janssen, Birgit Ertl-Wagner, Maximilian F. Reiser, Annika Plate, Andreas Straube, Louisa von Baumgarten

J Cereb Blood Flow Metab. 2016 Apr; 36(4):743-54

Impact factor 2016: 4,9

* geteilte Erstautorenschaft

Crossed cerebellar diaschisis in patients with acute middle cerebral artery infarction: Occurrence and perfusion characteristics

Wieland H Sommer^{1,*}, Christine Bollwein^{1,*}, Kolja M Thierfelder¹, Alena Baumann¹, Hendrik Janssen², Birgit Ertl-Wagner¹, Maximilian F Reiser¹, Annika Plate³, Andreas Straube³ and Louisa von Baumgarten³

Abstract

We aimed to investigate the overall prevalence and possible factors influencing the occurrence of crossed cerebellar diaschisis after acute middle cerebral artery infarction using whole-brain CT perfusion. A total of 156 patients with unilateral hypoperfusion of the middle cerebral artery territory formed the study cohort; 352 patients without hypoperfusion served as controls. We performed blinded reading of different perfusion maps for the presence of crossed cerebellar diaschisis and determined the relative supratentorial and cerebellar perfusion reduction. Moreover, imaging patterns (location and volume of hypoperfusion) and clinical factors (age, sex, time from symptom onset) resulting in crossed cerebellar diaschisis were analysed. Crossed cerebellar diaschisis was detected in 35.3% of the patients with middle cerebral artery infarction. Crossed cerebellar diaschisis was significantly associated with hypoperfusion involving the left hemisphere, the frontal lobe and the thalamus. The degree of the relative supratentorial perfusion reduction was significantly more pronounced in crossed cerebellar diaschisis-positive patients but did not correlate with the relative cerebellar perfusion reduction. Our data suggest that (i) crossed cerebellar diaschisis is a common feature after middle cerebral artery infarction which can robustly be detected using whole-brain CT perfusion, (ii) its occurrence is influenced by location and degree of the supratentorial perfusion reduction rather than infarct volume (iii) other clinical factors (age, sex and time from symptom onset) did not affect the occurrence of crossed cerebellar diaschisis.

Keywords

Crossed cerebellar diaschisis, CT perfusion imaging, ischemic stroke, MCA infarction

Received 17 May 2015; Revised 9 October 2015; Accepted 12 October 2015

Introduction

The first characterisation of ‘diaschisis’ traced back to von Monakow who described it in the 1870s as an ‘abolition of excitability’ and ‘functional standstill’ in an intact brain area distant from but linked to an area of cerebral damage. Baron et al.¹ transferred this concept in the 1980s to a phenomenon that was termed crossed cerebellar diaschisis (CCD). CCD refers to the association between a local supratentorial brain lesion and a simultaneous decrease of contralateral cerebellar blood flow and metabolic activity.² Current scientific concepts imply that interruption of corticopontocerebellar tracts causes a remote functional deactivation by a reduced

¹Institute for Clinical Radiology, Ludwig-Maximilians-University Hospital Munich, Munich, Germany

²Department of Neuroradiology, Ludwig-Maximilians-University Hospital Munich, Munich, Germany

³Department of Neurology, Ludwig-Maximilians-University Hospital Munich, Munich, Germany

*Both authors contributed equally to this paper

Corresponding author:

Louisa von Baumgarten, Department of Neurology, University of Munich Hospitals Grosshadern Campus, Marchioninistr 15, 81377 Munich, Germany.

Email: Louisa.vonBaumgarten@med.uni-muenchen.de

excitatory input and a decreased cerebellar flow.³ CCD was reported in chronic diseases, such as brain tumors⁴ but also as a result of acute circuit inactivation, for example after stroke^{5,6} and cerebral hemorrhage.⁷ The original definition of diaschisis was based on the notion that it was a transient and totally reversible event,⁸ whereas subsequent publications showed that it can persist for years and lead to irrevocable degeneration.^{9–11} In the first hours after stroke, however, it has been shown that diaschisis is potentially reversible if supratentorial reperfusion can be achieved.^{5,12} The pathophysiological concept of diaschisis is nowadays widely accepted and many articles concerning different aspects of this phenomenon have been published meanwhile. Controversies prevail, though, e.g. in regard to the frequency of CCD following different forms of supratentorial damage, its prognostic value, its dependency on the location and size of the supratentorial lesion and its clinical correlates.^{6,13,14}

Imaging studies on CCD have mainly involved nuclear medicine-based techniques like SPECT, PET and Xenon-computed tomography. All of them are used as reference methods for perfusion imaging but are not available in routine clinical care. Therefore, only small patient collectives have been evaluated with regard to CCD after acute supratentorial damage by these methods so far. Advances in imaging technology now allow whole-brain CT perfusion (WB-CTP),¹⁵ a method, which is becoming increasingly available and is part of the acute stroke workup in many centers. Using this methodology, it has been possible to robustly study the cerebellar perfusion¹⁶ and to detect CCD after acute supratentorial damage.^{7,17}

In our study, we screened a large patient cohort and aimed to (i) investigate the overall prevalence of CCD after acute infarction in the middle cerebral artery (MCA) territory using WB-CTP and to (ii) determine potential factors influencing the occurrence of CCD.

Materials and methods

Study population and patient selection

From March 2009 to January 2014, 1644 consecutive patients who were admitted to our institution for suspected stroke and who underwent emergency multimodal stroke CT were evaluated. The study was designed as a retrospective single-center study at a large university hospital. The institutional review board of the Ludwig-Maximilians University Munich (Ethikkommission der Medizinischen Fakultät der Ludwig-Maximilians Universität München) approved the study according to the Helsinki Declaration of 1975 (and as revised in 2013) and waived requirement

for informed consent. The final study population was selected according to the following criteria:

Inclusion criterion. Acute occlusion of the ICA, the carotid-T and/or the M1 and M2 segment of the MCA on CT angiography (CTA) with a concomitant perfusion deficit in the MCA territory on CTP

Exclusion criteria.

1. Absence of confirmed infarction of the MCA territory by follow-up CT/MRI.
2. Any abnormality of the vertebrobasilar arteries as determined by CTA (e.g. hypoplasia, stenosis, occlusion).
3. Any pathology of the cerebellum in non-enhanced CT (NECT) of the brain (e.g. prior ischemia, hemorrhage, tumor).
4. Cerebellar ischemia on follow-up CT/MRI.
5. CTP coverage of less than 50% of the cerebellum or poor image quality.

The study was designed as a case–control study with a ratio of cases to controls of 1:2 in order to prevent biased reading.¹⁸ WB-CTP datasets of the control group had no cerebrovascular abnormalities on WB-CTP as well as on follow-up MRI.

CT examination protocol

The CT imaging protocol consisted of a NECT to exclude intracerebral hemorrhage, a supra-aortic CTA and a WB-CTP. The examinations were performed on the following multislice CT scanners: SOMATOM Definition AS+, a 128 slice CT scanner; SOMATOM Definition Flash, a 128 slice dual source CT scanner; SOMATOM Definition Edge, a 128 slice CT scanner (all Siemens Healthcare, Erlangen, Germany). WB-CTP was acquired with 0.6 mm collimation and scan coverage of 100 mm in the z-axis by means of a toggling table technique. One scan was acquired every 1.5 s with the following imaging parameters: tube voltage 80 kV; tube current 200 mAs; and CTDI_{vol} 276.21 mGy. Thirty-five millilitres of highly iodinated contrast agent were administered intravenously at a flow rate of 5 ml/s, followed by a saline flush of 40 ml at 5 ml/s; Axial slices (31) with a thickness of 10 mm and an increment of 3 mm were reconstructed from the dataset.

CT perfusion image processing

The processing of source images was performed with the SYNGO Volume Perfusion CT Neuro software using a semi-automated deconvolution algorithm (Auto Stroke MTT) on a dedicated workstation

(Syngo MMWP, VA 21A; Siemens Healthcare, Erlangen, Germany). The arterial input function was selected as described earlier.¹⁹ Briefly, a vendor given algorithm was used to select a region of interest (ROI) within the earliest-appearing arteries at a representative slice at the level of the basal ganglia. The venous output region was selected from the superior sagittal sinus. A series of 31 color-coded slices was generated for each of the hemodynamic parameters cerebral blood flow (CBF), cerebral blood volume (CBV), mean transit time (MTT), time to drain (TTD) and time to peak (TTP). CBV is the whole amount of blood in a defined unit of tissue. In contrast to CBV, CBF, MTT, TTP and TTD are related to the passage of blood in a given time window. Due to changes in the software features during the period of data acquisition (2009–2014), MTT, TTD and TTP were not available for all but in 99.0%, 87.7% and 24.0% of the patients, respectively. CBF and CBV were assessed for all datasets. The color slices were saved in DICOM format and displayed on default window settings for further evaluation.

Follow-up imaging

For patients with MCA infarction, follow-up imaging consisted of MRI in 88 (56.4%) patients and NECT in 68 (43.6%) patients, respectively. The MRI follow-up examination comprised a T2* sequence, a fluid-attenuated inversion recovery (FLAIR) sequence, a diffusion-weighted imaging (DWI) sequence and a time-of-flight (TOF)-MR angiography. The median time delay between CT perfusion scan and follow-up imaging was two days (range: 1–49 days) for MRI and one day (range: 1–16 days) for NECT.

Image analysis

Initially, a study population was created by random selection of patients ($N_p = 156$) and controls with a ratio of 1:2. Subsequently, the respective CTP data sets (CBF, CBV, MTT, TTD and TTP) were converted into JPEG files and inserted into PowerPoint (Microsoft PowerPoint 2013, Microsoft Co., Redmond/US-WA) for further processing. The JPEG files were saved in the default format without the possibility of changing the window setting. All images were presented to the readers after having been cropped to an extent that only the cerebellar, but not the supratentorial brain parenchyma was visible (performed by CB). The assessment of presence/absence of CCD was subsequently performed qualitatively by two independent raters (one neurologist with eight years (LvB) and one radiologist with seven years (WS) of experience in CTP reading, respectively) who were blinded to the clinical data.

In case of disagreement, a consensus was reached in a separate session.

In the following analysis, only perfusion anomalies in the cerebellar hemisphere contralateral to the supratentorial lesion were counted as CCD positive. CCD was rated positive if at least two of the perfusion maps (irrespective of which parameters) showed a deficit on the same side. This approach has already been applied by Thierfelder et al.^{16,20} with the objective of achieving valid results for both sensitivity and specificity.

The degree and extent of the supratentorial ischemic lesion on admission were quantified on each of the existing CTP maps by applying the Alberta stroke program early computed tomography score for CT perfusion (CTP-ASPECTS), a topographical scoring system, which provides localisation-weighted values ranging from 0 to 10.²¹ Additionally, we extended the ASPECT score by adding the thalamus as a further anatomical region of interest, as a perfusion deficit in this location was described to be relevant for the induction of cerebellar diachisis.^{22,23}

Final infarct volume was determined either on follow-up MR or on follow-up NECT using a volumetric approach as previously described.¹⁹ Briefly, regions of interest around the infarct lesions were delineated on all relevant slices using OsiriX (OsiriX V.4.0 imaging software 2011) on a 27-in. iMac computer (Apple Inc., Cupertino, CA, USA). Infarct volume was calculated in cm^3/ml by multiplying the areas by the slice thickness.

The software Syngo.via Single Sign On (Siemens Healthcare, Erlangen, Germany) was used for the calculation of the absolute perfusion values based on the raw data which were still available for 116 of 156 patients (74.4%). We chose a semi-quantitative approach, which was described previously.¹⁷ Briefly, the area of the abnormal perfusion was segmented manually in the affected hemisphere, and subsequently was mirrored to the contralateral hemisphere. A representative slice, showing the greatest interhemispheric difference was chosen and differences in the absolute perfusion parameters were determined. The same procedure was adopted for the cerebellar hemispheres. Here, circular ROIs were used to obtain quantitative perfusion values.

Perfusion asymmetry was assessed as follows:

$$\begin{aligned} \text{Cerebrum: } & \frac{\text{TTD}_{\text{ipsilateral}} - \text{TTD}_{\text{contralateral}}}{\text{MTT}_{\text{ipsilateral}} - \text{MTT}_{\text{contralateral}}} \\ & \frac{(\text{CBF}_{\text{contralateral}} - \text{CBF}_{\text{ipsilateral}}) / \text{CBF}_{\text{contralateral}} \times 100\% \text{ (CBF reduction rate)}}{(\text{CBV}_{\text{contralateral}} - \text{CBV}_{\text{ipsilateral}}) / \text{CBV}_{\text{contralateral}} \times 100\% \text{ (CBV reduction rate)}} \\ \text{Cerebellum: } & \frac{\text{TTD}_{\text{contralateral}} - \text{TTD}_{\text{ipsilateral}}}{\text{MTT}_{\text{contralateral}} - \text{MTT}_{\text{ipsilateral}}} \end{aligned}$$

$$\frac{(CBF_{\text{ipsilateral}} - CBF_{\text{contralateral}})}{CBF_{\text{ipsilateral}}} \times 100\% \text{ (CBF reduction rate)}$$

$$\frac{(CBV_{\text{ipsilateral}} - CBV_{\text{contralateral}})}{CBV_{\text{ipsilateral}}} \times 100\% \text{ (CBV reduction rate)}$$

Statistical analysis

All statistical analyses were performed using Excel (Microsoft Excel 2013, Microsoft Co., Redmond/US-WA) and MedCalc (MedCalc Software, Ostend/Belgium). On the basis of the two independent readings, the degree of inter-rater agreement in the evaluation of perfusion maps was assessed by calculation of the Kappa coefficient. In addition, the proportion of patients with MCA infarct diagnosed as CCD positive was determined in general and for each of the perfusion parameters. To test for normal distribution the Shapiro-Wilk test was performed. Given a non-normal distribution, we applied the Mann-Whitney-U test to identify significant differences between patients classified as CCD positive and CCD negative classified patients. The association between CCD and the presence of ischemic lesions on CTP in the predefined anatomical cerebral regions was elucidated by use of the Chi-squared test and Fisher's exact test. The Spearman's rank correlation was used to analyse the relationship between supra- and infratentorial perfusion values. The significance level for all tests was set

at $P < 0.05$. In case of multiple testing, the significance level was adjusted according to Bonferroni. Data are expressed as mean \pm standard deviation/95% confidence interval or as median \pm interquartile range depending on the distribution of data.

Results

Patient characteristics

The final patient cohort consisted of 156 individuals who were included in the further analysis. The patient flow chart is illustrated in Figure 1. Mean age (\pm SD) was 69.7 years (\pm 14.9) and 63.3 years (\pm 15.8) in the patient group and in the control group, respectively. The patient group included 69 male subjects (44%) compared with 87 in the control group (56%). Time from symptom onset did not differ significantly between the cohorts (228 ± 213 min vs. 218 ± 323 min, $P = 0.7471$). In the patient group, MCA infarcts were located in the left cerebral hemisphere in 52.6% of cases. Mean final infarct volume (\pm SD) was 56.5 ml (\pm 86.6) and median ASPECTS score was 3 (interquartile range: 1–6). The most common diagnoses in the control group included transient ischemic attacks (44.5%), epileptic seizures (16.1%), encephalitis/myelitis/meningitis (5.8%), encephalopathy (5.2%) and cerebral hemorrhage (3.9%). Patient characteristics are summarised in Table 1.

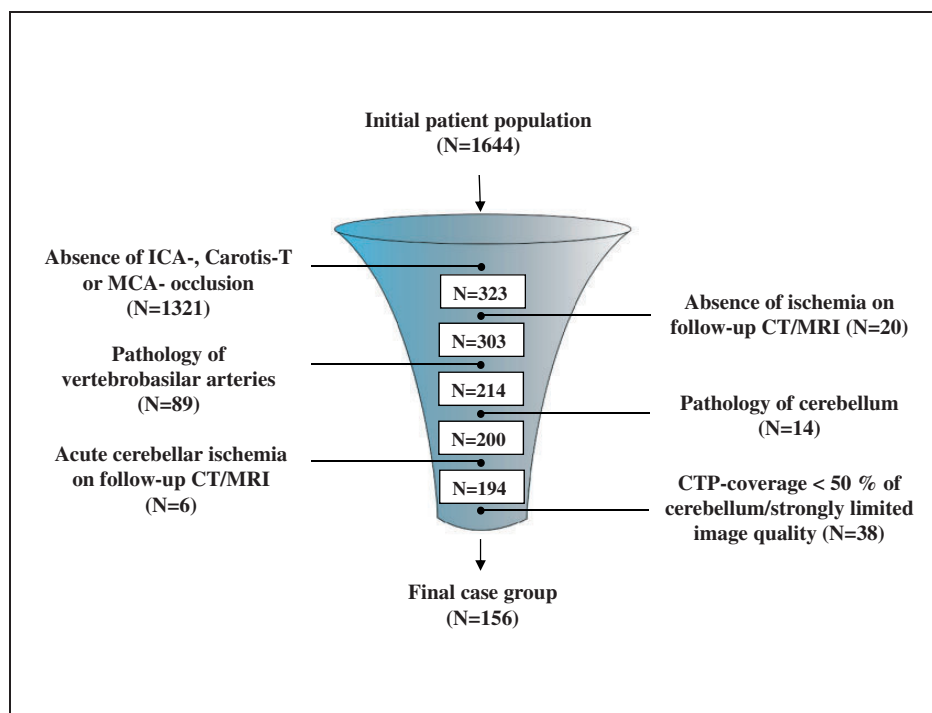


Figure 1. Patient selection.

Table 1. Characteristics of the study population.

	Patient group		Control group	
	Value	Range	Value	Range
N	156		312	
Age (years) \pm SD	69.7 \pm 14.9	28–97	63.3 \pm 15.8	27–110
Male gender (%)	44	–	56	–
Time from symptom onset (min) \pm SD	228 \pm 213 ^a	34–1356	218 \pm 323 ^b	53–2462
Infarction on left hemisphere (%)	52.6	–	–	–
ASPECTS (median) \pm interquartile range	3 \pm 1/6	0–10	–	–
Final infarction volume (ml) \pm SD	74.9 \pm 100.4	0.1–496.1	–	–

SD: standard deviation; ASPECTS: Alberta stroke program early computed tomography score. ^aAvailable for 60.3% of subjects. ^bAvailable for 41.0% of subjects.

Table 2. Proportion of CCD+ and CCD– cases among the patient and control group.

	CCD+	CCD–	P
Patient group (N = 156)	55 (35.3%)	101 (64.7%)	<0.0001 ^a
Control group (N = 312)	39 (12.5%)	273 (87.5%)	

CCD: crossed cerebellar diaschisis. ^aStatistically significant (Chi-squared test).

Inter-rater agreement

We assessed the inter-rater agreement in the detection of CCD. The kappa statistic calculated by means of the two independent readings yielded a value of 0.73 which can be interpreted as a good degree of agreement.²⁴

Frequency of CCD

The number of CCD-positive and CCD-negative CTP maps was determined on the basis of the consensus reading. Results are illustrated in Table 2. Within the patient group, 55/156 (35.3%) subjects were rated CCD positive, while 101/156 (64.7%) subjects were diagnosed as CCD negative. Among controls, 39 CTP maps (12.5%) were rated false-positive for CCD, while the remaining 273 CTP maps (87.5%) were correctly identified as CCD negative. CCD was detected with a significantly higher frequency in the presence of MCA infarction than in controls (35.5% vs. 12.5%, $P < 0.0001$).

The CTP map with the highest detection rate of CCD among the subjects with MCA infarct was CBF (35.0%), followed by TTD (31.4%), CBV (26.3%), MTT (22.4%) and TTP (17.5%). For the differentiation between CCD positive and negative cases, TTP showed a high diagnostic value of 98.6%. Similarly, CBV performed considerably well with 94.2%, while the other parameters CBF (87.3%), TTD (85.5%) and MTT (85.5%) ranged at a lower level. Figure 2 shows three representative examples of CCD-positive examinations.

Determining factors for the occurrence of CCD

Among patients with MCA infarction, we analysed factors with potential influence on the occurrence of CCD. Results are presented in Table 3. A left-sided MCA infarction was significantly associated with the occurrence of CCD (CCD positive: 56.4% left hemisphere vs. 43.6% right hemisphere; CCD negative: 50.5% left hemisphere vs. 49.5% right hemisphere, $P = 0.0427$). A higher mean ASPECTS score was found for CCD-positive patients (2.6 (2.0;3.1) for CCD positive vs. 3.5 (3.0;4.0) for CCD negative, $P = 0.0283$). Other variables ('time from symptom onset to CT examination', 'age', 'gender' and 'volume of supratentorial infarction') did not reach the predefined level of significance of $P < 0.05$. After the Bonferroni correction for multiple testing, only a left-sided infarction but not the ASPECTS score remained statistically significant.

Dichotomised univariate associations between infarct locations as assessed by ASPECTS and CCD were explored by applying the Chi-squared test to the data of MCA-infarct patients. Results are shown in Table 4. Cerebral hypoperfusion involving the following territories were significantly associated with CCD: M 1 (anterior MCA cortex; CCD-positive examinations: 94.5% vs. CCD-negative examinations: 80.2%, $P = 0.0175$), M 4 (anterior MCA territory superior to M 1) (CCD positive: 98.2% vs. CCD negative: 82.2%, $P = 0.0036$), the internal capsule (CCD positive: 67.3% vs. CCD negative: 44.6%, $P = 0.0109$) and the thalamus (CCD positive: 69.1% vs. CCD negative: 33.7%, $P < 0.0001$). No significant association was detected for other cortical regions (insula, M 2: cortex lateral to insular ribbon, M 3: posterior MCA cortex, M 5: lateral MCA territory superior to M 2, M 6: posterior MCA territory superior to M 3) and subcortical regions (caudate nucleus, lentiform nucleus). After a Bonferroni correction for multiple testing, only the thalamus and the ASPECTS-defined region M4 which

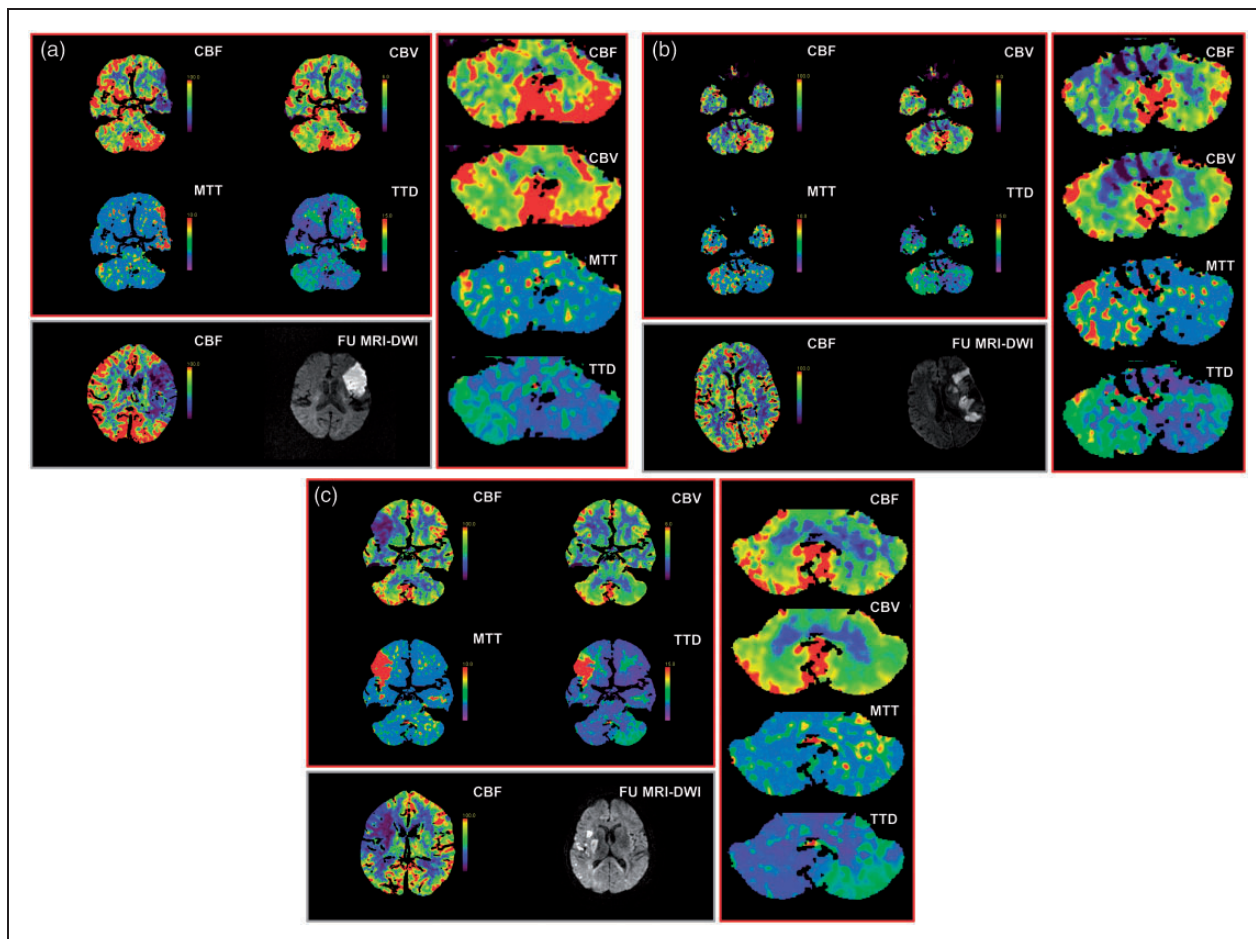


Figure 2. Representative cases of MCA infarction and CCD are shown in Figure 2 (a–c). CTP maps (CBF, CBV, MTT and TTD, right panel: higher resolution) of the cerebellar perfusion on admission are shown in the red frame. The infarcted tissue (CBF upon admission, corresponding follow-up MRI-DWI) is demonstrated within the grey frame. (a) Ninety year-old woman with acute right-sided hemiparesis, left-sided gaze preference and expressive aphasia. Time from symptom onset to CTP imaging was 75 min and to MRI follow-up 67 h, respectively. (b) Sixty-nine year-old woman with acute right-sided hemiparesis and global aphasia. Time from symptom onset to CTP imaging was 150 min and to follow-up MRI 71 h, respectively. (c) Sixty-five year-old woman with acute left-sided hemiplegia, dysarthria and a neglect. Time from symptom onset to CTP imaging was 120 min and to follow-up MRI 100 h. In all patients, rtPA was administered immediately after CT workup.

is located in the frontal lobe remained statistically significant. Figures 2(c) and, in more detail, Figure 3 show examples of an ipsilateral thalamic hypoperfusion in a patient with CCD.

Quantitative analysis of perfusion values

Quantification of the relative supratentorial cerebral perfusion parameters revealed that that MTT and TTP prolongation as well as CBF reduction is more pronounced in CCD-positive patients than in CCD-negative patients (Table 5). Significant differences between CCD-positive and -negative patients could be detected for MTT (0.48 (0.09;0.75) for CCD positive vs. 0.10 (0.19;0.43) for CCD negative; $P=0.0005$), TTD (0.62 (0.30;1.04) for CCD positive vs. 0.33

(−0.04;0.61) for CCD negative; $P=0.0017$) and CBF (19.28 (15.78;26.69) for CCD positive vs. 14.15 (4.66;21.75) for CCD negative; $P=0.0032$). CBV, however, showed no significant difference between these groups (11.67 (7.98;18.34) for CCD positive vs. 11.86 (3.68;20.31) for CCD negative; $P=0.9217$).

Among CCD-positive cases, no significant correlation could be detected between the degree of the supratentorial perfusion and the cerebellar perfusion reduction (Table 6).

Discussion

WB-CTP offers a robust method to screen for CCD in a large patient collective. In our cohort, perfusion abnormalities of the cerebellum consistent with CCD

Table 3. Comparison of clinical features and infarct variables between CCD+ and CCD- cases.

	CCD+ (N = 55)	CCD- (N = 101)	P
Volume of supratentorial infarction (ml) ^a	81.3 (55.6;107.0)	71.4 (51.0;91.9)	0.1297 ^b
Supratentorial infarction of left hemisphere (%)	56.4	50.5	0.0427 ^{c,d}
ASPECTS ^a	2.6 (2.0;3.1)	3.5 (3.0;4.0)	0.0283 ^{b,d}
Time from symptom onset (min) ^a	205.5 (146.2;264.8)	239.7 (174.9;304.5)	0.5622 ^b
Age (years) ^a	67.0 (63.7;70.4)	72.4 (68.5;76.2)	0.0815 ^b
Male gender (%)	45.5	43.6	0.9534 ^c

CCD: crossed cerebellar diaschisis; ASPECTS: Alberta stroke program early computed tomography score. ^aValues are mean (95% confidence interval). ^bMann-Whitney test. ^cChi-squared test. ^dStatistically significant.

Table 4. Influence of supratentorial infarct location on the incidence of CCD.

Anatomical structures involved in supratentorial infarction		CCD+ (N = 55)	CCD- (N = 101)	P
A S P E C T S	Caudate nucleus	63.6% (35/55)	51.5% (52/101)	0.1966 ^a
	Lentiform nucleus	63.6% (35/55)	56.4% (57/101)	0.4819 ^a
	Internal capsule	67.3% (37/55)	44.6% (45/101)	0.0109 ^a
	Insula	94.6% (52/55)	90.1% (91/101)	0.5453 ^b
	M 1	94.6% (52/55)	80.2% (81/101)	0.0175 ^b
	M 2	98.2% (54/55)	92.1% (93/101)	0.1610 ^b
	M 3	92.7% (51/55)	83.2% (84/101)	0.1396 ^b
	M 4	98.2% (54/55)	82.2% (83/101)	0.0036 ^{b,c}
	M 5	98.2% (54/55)	94.1% (95/101)	0.4225 ^b
Thalamus	69.1% (38/55)	33.7% (34/101)	< 0.0001 ^{a,c}	

CCD: crossed cerebellar diaschisis; ASPECTS: Alberta stroke program early computed tomography score. ^aChi-squared test. ^bFisher's exact test. ^cStatistically significant.

were observed in 35.3% of all patients. The perfusion parameters CBF and TTD reached the highest detection rates, whereas TTP and CBV best distinguished between CCD-positive and -negative cases. The location of the supratentorial perfusion deficit, rather than its size, as well as the severity of cerebral hypoperfusion was decisive for the occurrence of CCD. We could show that a location on the left side, in the frontal lobe and the thalamus is associated with the evolution of CCD.

The frequency of CCD after MCA infarction in our study lies within the published range of CCD after supratentorial strokes (15.61%–46.2%).^{13,14,22,25–27} The results of these studies, however, were predominantly obtained by analyses of small study populations (range: 18–113)^{13,14,17,22,25,26,28} and/or by inclusion of various vascular territories^{1,13,25,27–29} and by inclusion of acute and chronic infarcts.^{26,27} The strokes we investigated, however, were acute strokes restricted to the MCA territory to avoid a dispersion of the results by inclusion of different infarct stages and vascular territories. By screening a large patient collective, we can

thus further extend and substantiate the observation that CCD is a common phenomenon after MCA infarction and that WB-CTP provides an appropriate tool to investigate its hemodynamic impact on cerebellar perfusion after cerebral infarction.

In our study, we found a high rate of thalamic hypoperfusion in patients with MCA stroke. In principle, occlusions of the internal carotid artery could lead to an insufficient thalamic blood supply via the posterior communicating artery as well as via the anterior choroidal artery. However, blood flow via the contralateral side should compensate for this deficit, and thalamic infarction usually relates to infarctions of the tuberothalamic artery (arising from the posterior communicating artery), the paramedian, the inferolateral artery or the posterior choroidal artery (arising from the posterior cerebral artery).³⁰ In our study, ipsilateral thalamic perfusion alterations were also observed in patients without carotid occlusion (data not shown). Notably, in all cases with an ipsilateral thalamic perfusion alteration on the initial CTP, no thalamic infarction was detected in the follow-up imaging.

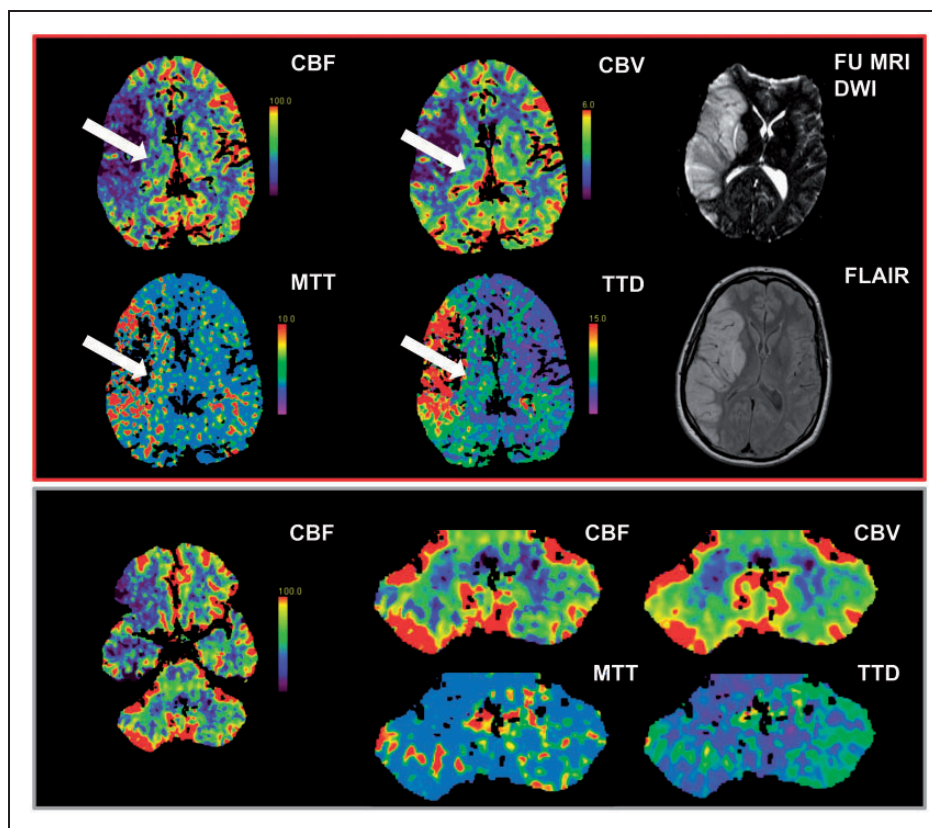


Figure 3. A representative case of MCA infarction, ipsilateral thalamic hypoperfusion and CCD is shown in Figure 3. CTP maps (CBF, CBV, MTT and TTD) of the supratentorial perfusion including the thalamus as well as the respective follow-up MRI (DWI and FLAIR) are shown in the red frame. White arrows indicate the area of thalamic hypoperfusion. The cerebellar hypoperfusion (left side: CBF, right side: higher resolution CBF, CBV, MTT and TTD) are shown in the gray frame. Images were obtained from a 48 year-old male with acute left-sided hemiparesis due to a right-sided MI-occlusion. Time from symptom onset to CTP imaging was 190 min and to MRI follow-up 64 h, respectively. After CT-workup, rtPA was administered immediately and subsequent (successful) mechanical recanalisation of the MI-segment was performed.

Table 5. Comparison of supratentorial perfusion reduction between CCD+ and CCD- cases.

Cerebral perfusion parameters	CCD+ (N = 43) Median (95% CI)	CCD- (N = 73) Median (95% CI)	P
Δ MTT (s)	0.48 (0.09;0.76)	0.10 (-0.19;0.43)	0.0005^a
Δ TTD (s)	0.62 (0.30;1.04)	0.33 (-0.04;0.61)	0.0017^a
CBV reduction rate (%)	11.67 (7.98;18.34)	11.86 (3.68;20.31)	0.9217
CBF reduction rate (%)	19.28 (15.78;26.69)	14.15 (4.66;21.75)	0.0032^a

MTT: mean transit time; TTD: time to drain; CBF: cerebral blood flow; CBV: cerebral blood volume. Δ MTT: $MTT_{ipsilateral} - MTT_{contralateral}$; Δ TTD: $TTD_{ipsilateral} - TTD_{contralateral}$; CBV reduction rate: $(CBV_{contralateral} - CBV_{ipsilateral}) / CBV_{contralateral} \times 100\%$; CBF reduction rate: $(CBF_{contralateral} - CBF_{ipsilateral}) / CBF_{contralateral} \times 100\%$, ^aStatistically significant.

According to the literature, not only cerebellar diachisis but also ipsilateral thalamic hypoperfusion have been described after cortical³¹ and capsular³² infarctions in rats and after MCA infarctions in humans.^{33,34} Similarly, in status epilepticus, diffusion restrictions indicating CCD as well as an ipsilateral thalamic

involvement have been described.^{35,36} Furthermore, crossed cerebello-thalamo-cerebral diachisis as indicated by an FDG hypometabolism in the contralateral thalamus and cerebral cortex has been reported after acute cerebellar injury using FDG-PET.³⁷ Therefore, the observed perfusion alteration in the

Table 6. Correlation of cerebral and cerebellar perfusion parameters in CCD+ cases.

	Spearman's Rho correlation coefficient (P)			
	Cerebellar Δ MTT	Cerebellar Δ TTD	Cerebellar CBV reduction rate	Cerebellar CBF reduction rate
Cerebral Δ MTT	0.132 (0.399)	0.275 (0.074)	0.049 (0.758)	0.155 (0.321)
Cerebral Δ TTD	0.132 (0.398)	0.107 (0.494)	0.090 (0.565)	0.198 (0.204)
Cerebral CBV reduction rate	0.097 (0.538)	0.052 (0.742)	-0.027 (0.862)	0.051 (0.744)
Cerebral CBF reduction rate	0.302 (0.049)	0.370 (0.015)	0.021 (0.892)	0.232 (0.134)

MTT: mean transit time; TTD: time to drain; CBF: cerebral blood flow; CBV: cerebral blood volume. Cerebral Δ MTT: $MTT_{ipsilateral} - MTT_{contralateral}$, Cerebral Δ TTD: $TTD_{ipsilateral} - TTD_{contralateral}$, Cerebral CBV reduction rate: $(CBV_{contralateral} - CBV_{ipsilateral})/CBV_{contralateral} \times 100\%$, Cerebral CBF reduction rate: $(CBF_{contralateral} - CBF_{ipsilateral})/CBF_{contralateral} \times 100\%$, Cerebellar Δ MTT: $MTT_{contralateral} - MTT_{ipsilateral}$, Cerebellar Δ TTD: $TTD_{contralateral} - TTD_{ipsilateral}$, Cerebellar CBV reduction rate: $(CBV_{ipsilateral} - CBV_{contralateral})/CBV_{ipsilateral} \times 100\%$, Cerebellar CBF reduction rate: $(CBF_{ipsilateral} - CBF_{contralateral})/CBF_{ipsilateral} \times 100\%$.

thalamus most likely relates to an ipsilateral thalamic diachisis.

According to current knowledge, the interruption of fiber tracts projecting via pontine nuclei to the contralateral cerebellar cortex and to the deep cerebellar nuclei lead to a reduced activation of the cortical Purkinje cells as well as a reduced activity of glutamnergic projection neurons from the deep cerebellar nuclei to the thalamus.^{38,39} This results in a functional deactivation and ultimately to vasoconstriction which in turn results in a profound reduction of CBF and CBV.⁴⁰

The relatively high detection rate of CBF in comparison to the other perfusion parameters supports this theory. Due to the concomitant reduction of CBF and CBV, changes in time-based perfusion maps are not expected.⁴¹ However, we and others,^{7,27} do indeed find alterations in time-based MRI²⁷ and CTP-based perfusion maps like MTT, TTP and TTD.^{7,17} Importantly, we ruled out that the perfusion changes in the time-dependent maps are related to vascular disease or ischemia in the posterior circulation.

In the literature, disagreement exists whether infarction volume influences CCD occurrence and severity. Kim et al.¹³ reported that the location rather than the extent or severity of the lesion may be the major determinant for the occurrence and magnitude of CCD in patients with cerebral infarction. Sobesky et al.,⁵ however, found that acute but not chronic CCD was closely related to the volume of supratentorial hypoperfusion. Lin et al.²⁷ showed in a small study that infarct volume is related to the development of CCD. In our study on acute MCA stroke, however, we could find no association between infarct size and occurrence of CCD. In this study, we could demonstrate that a more pronounced supratentorial perfusion alteration seen in MTT, TTD or CBF is positively correlated with the evolution of CCD, which is in line with a previous

SPECT study demonstrating that the degree of hypoperfusion is correlated with the occurrence of CCD.²⁵ However, we did not find a correlation between the degree of the supratentorial perfusion alteration and the degree of the cerebellar hypoperfusion.

Cerebral hypoperfusion in the frontal lobe and the thalamus were associated with CCD which is in agreement with previously published results of smaller collectives.^{10,13,22,29,42,43} Pantano et al.⁴⁴ demonstrated that CCD was more prominent when the supratentorial infarct involved the internal capsule or the cortical mantle extensively. They also suggested that destruction of the pyramidal tract is neither necessary nor sufficient to induce CCD. Gold and Lauritzen³ showed that decreases of activity involving the frontal cortex produced the largest decrease in contralateral cerebellar electrical activity and blood flow. It has been shown that small infarcts, if located in a strategically relevant thalamic area (e.g. nucleus ventralis intermedius), are sufficient to elicit a relevant decrease of the contralateral cerebellar blood flow and metabolism.^{22,23} Overall, these data are in line with our observation that there is an association between anatomic region and the incidence of CCD which is not the case for the size of the cerebellar hypoperfusion.

The structural basis accounting for the development of CCD by cerebral hypoperfusion involving the frontal lobe and the thalamus might be the dentatorubrothalamic pathway, specific thalamic projections and the corticopontocerebellar tract.^{23,45} Furthermore, it is known that the cerebellar-cortical pathways are structured in reciprocal organised loops and that the cerebellar hemispheres in particular are interconnected to the frontal cortex.⁴⁶ In our cohort, a significantly higher proportion of CCD occurred after left-sided MCA infarctions. This observation may indicate that frontothalamocerebellar circuits which are supposed to be intricately involved in language,⁴⁷ complex motor

functions,⁴⁸ verbal working performance⁴⁹ account for the development of CCD. Based on our findings, it can be suggested that the amount of interconnection of frontal cortex and cerebellar hemisphere is more intense for the left frontal cortex.

Subacute neurologic function and recovery have been shown to be worse in patients with stroke and CCD compared with those without CCD.⁵⁰ Although no reports to date show that cerebellar hypoperfusion from CCD is associated with permanent infarction, chronic deafferentation results in measurable structural abnormalities.⁵¹ A serial PET study with longitudinal follow-up at multiple time points after thrombolytic therapy also highlighted the usefulness of CCD as an indicator of clinical outcomes.⁵ Our data indicate that WB-CTP evaluation might be a potent tool to clarify the role of CCD for patient outcome after MCA infarction.

Our data must be interpreted in the context of the study design. This is a retrospective single-center study on the occurrence of CCD after MCA infarction which is based on a dichotomised univariate descriptive statistical analysis. Consequently, no exact predictions but only significant associations can be revealed by our investigations. We did not analyse the potential impact of CCD on patient's clinic or outcome, although these are important aspects for future studies. However, our study demonstrates that such studies could well be performed using the WB-CTP. We blinded our readers to clinical data and presence of a supratentorial infarction to minimise bias. Moreover, we enrolled a large patient cohort which exceeded the size of study populations investigated in terms of CCD so far (mean: 51.1; range: 18–113).^{13,14,17,22,25,26,28,52} Still, we cannot fully rule out the possibility of having underestimated the frequency of CCD as we counted only those cases as CCD positive, that show hemodynamic alterations suggestive of CCD in at least two perfusion parameter maps. However, artifacts on single perfusion maps can often be observed in CT imaging of the posterior fossa and this approach helped to limit the number of false-positive findings.

Moreover, the sensitivity might have been negatively influenced by the fact that JPEGs of the raw perfusion maps were presented to the readers which could not be windowed for brightness and contrast. The JPEG files, however, allowed us to easily modify the images to blind the readers to the supratentorial brain sections.

CTP alterations suggestive of CCD were also observed in subjects of the control group. These might be related to artifacts. Moreover, transient ischemic attacks or epileptic seizures, two of the two main reasons for admission within the control group, could

potentially result in CCD and cause a substantial rate of false-positive results.

Conclusion

CCD is a common phenomenon after MCA infarcts and leads to a cerebellar hypoperfusion which can be detected by decreased CBF, CBV and/or by prolonged TTP, TTD and MTT. This phenomenon needs to be considered when interpreting CTP in acute supratentorial stroke in order to correctly classify contralateral cerebellar perfusion deficits. Prospective studies with larger cohorts and profound clinical assessment are necessary in order to further determine the clinical relevance of the observed phenomenon. In particular, patient relevant aspects like the immediate and long-term clinical correlates of CCD and its potential influence on outcome need to be subject of further research. For this purpose, an analysis of the WB-CTP images performed for the initial stroke workup seems to be a robust way to screen for CCD.

Funding

The author(s) received no financial support for the research, authorship, and/or publication of this article.

Declaration of conflicting interests

The author(s) declared no potential conflicts of interest with respect to the research, authorship, and/or publication of this article.

Authors' contributions

WHS and CB: contributed equally to this article. Conceived and designed the experiments: LVB, WHS. Performed the experiments: CB, AB, LVB, WHS. Analysed the data: CB, AB, WHS, LVB. Wrote (and revised) the manuscript: WHS, CB, LVB, AP, KMT, AS, MFR, JH, BEW.

References

1. Baron JC, Bousser MG, Comar D, et al. Crossed cerebellar diaschisis" in human supratentorial brain infarction. *Trans Am Neurol Assoc* 1981; 105: 459–461.
2. Baron JC, Rougemont D, Soussaline F, et al. Local interrelationships of cerebral oxygen consumption and glucose utilization in normal subjects and in ischemic stroke patients: a positron tomography study. *J Cereb Blood Flow Metab* 1984; 4: 140–149.
3. Gold L and Lauritzen M. Neuronal deactivation explains decreased cerebellar blood flow in response to focal cerebral ischemia or suppressed neocortical function. *Proc Natl Acad Sci USA* 2002; 99: 7699–7704.
4. Kajimoto K, Oku N, Kimura Y, et al. Crossed cerebellar diaschisis: a positron emission tomography study with 1-[methyl-11c]methionine and 2-deoxy-2-[18f]fluoro-d-glucose. *Ann Nucl Med* 2007; 21: 109–113.

5. Sobesky J, Thiel A, Ghaemi M, et al. Crossed cerebellar diaschisis in acute human stroke: a pet study of serial changes and response to supratentorial reperfusion. *J Cereb Blood Flow Metab* 2005; 25: 1685–1691.
6. Infeld B, Davis SM, Lichtenstein M, et al. Crossed cerebellar diaschisis and brain recovery after stroke. *Stroke* 1995; 26: 90–95.
7. Fu J, Chen WJ, Wu GY, et al. Whole-brain 320-detector row dynamic volume CT perfusion detected crossed cerebellar diaschisis after spontaneous intracerebral hemorrhage. *Neuroradiology* 2015; 57: 179–187.
8. Kempinsky WH. Vascular and neuronal factors in diaschisis with focal cerebral ischemia. *Res Publ Assoc Res Nerv Ment Dis* 1966; 41: 92–115.
9. Kim J, Lee SK, Lee JD, et al. Decreased fractional anisotropy of middle cerebellar peduncle in crossed cerebellar diaschisis: diffusion-tensor imaging-positron-emission tomography correlation study. *AJNR Am J Neuroradiol* 2005; 26: 2224–2228.
10. Mewasingh LD, Christiaens F, Aeby A, et al. Crossed cerebellar diaschisis secondary to refractory frontal seizures in childhood. *Seizure* 2002; 11: 489–493.
11. Tien RD and Ashdown BC. Crossed cerebellar diaschisis and crossed cerebellar atrophy: correlation of MR findings, clinical symptoms, and supratentorial diseases in 26 patients. *AJR Am J Roentgenol* 1992; 158: 1155–1159.
12. Hung YC, Chou YS, Chang CH, et al. Early reperfusion improves the recovery of contralateral electrophysiological diaschisis following focal cerebral ischemia in rats. *Neurol Res* 2010; 32: 828–834.
13. Kim SE, Choi CW, Yoon BW, et al. Crossed-cerebellar diaschisis in cerebral infarction: Technetium-99m-hmpao SPECT and MRI. *J Nucl Med* 1997; 38: 14–19.
14. De Reuck J, Decoo D, Lemahieu I, et al. Crossed cerebellar diaschisis after middle cerebral artery infarction. *Clin Neurol Neurosurg* 1997; 99: 11–16.
15. Morhard D, Wirth CD, Fesl G, et al. Advantages of extended brain perfusion computed tomography: 9.6 cm coverage with time resolved computed tomography-angiography in comparison to standard stroke-computed tomography. *Invest Radiol* 2010; 45: 363–369.
16. Thierfelder KM, Baumann AB, Sommer WH, et al. Vertebral artery hypoplasia: frequency and effect on cerebellar blood flow characteristics. *Stroke* 2014; 45: 1363–1368.
17. Jeon YW, Kim SH, Lee JY, et al. Dynamic CT perfusion imaging for the detection of crossed cerebellar diaschisis in acute ischemic stroke. *Korean J Radiol* 2012; 13: 12–19.
18. Rothman KJ. *Epidemiology: An introduction*. New York; Oxford: Oxford University Press, 2012.
19. Thierfelder KM, Sommer WH, Baumann AB, et al. Whole-brain CT perfusion: reliability and reproducibility of volumetric perfusion deficit assessment in patients with acute ischemic stroke. *Neuroradiology* 2013; 55: 827–835.
20. Thierfelder KM, von Baumgarten L, et al. Diagnostic accuracy of whole-brain computed tomographic perfusion imaging in small-volume infarctions. *Invest Radiol* 2014; 49: 236–242.
21. Parsons MW, Pepper EM, Chan V, et al. Perfusion computed tomography: prediction of final infarct extent and stroke outcome. *Ann Neurol* 2005; 58: 672–679.
22. Forster A, Kerl HU, Goerlitz J, et al. Crossed cerebellar diaschisis in acute isolated thalamic infarction detected by dynamic susceptibility contrast perfusion MRI. *PLoS One* 2014; 9: e88044.
23. Engelborghs S, Pickut BA, Marien P, et al. Crossed cerebellar diaschisis and hemiataxia after thalamic hemorrhage. *J Neurol* 2000; 247: 476–477.
24. Grouven U, Bender R, Ziegler A, et al. Der kappa-koeffizient. *Dtsch Med Wochenschr* 2007; 132: 65–68.
25. Nocun A, Wojczal J, Szczepanska-Szerej H, et al. Quantitative evaluation of crossed cerebellar diaschisis, using voxel-based analysis of Tc-99m ECD brain SPECT. *Nucl Med Rev Cent East Eur* 2013; 16: 31–34.
26. Komaba Y, Mishina M, Utsumi K, et al. Crossed cerebellar diaschisis in patients with cortical infarction: logistic regression analysis to control for confounding effects. *Stroke* 2004; 35: 472–476.
27. Lin DD, Kleinman JT, Wityk RJ, et al. Crossed cerebellar diaschisis in acute stroke detected by dynamic susceptibility contrast MR perfusion imaging. *AJNR Am J Neuroradiol* 2009; 30: 710–715.
28. Madai VI, Altaner A, Stengl KL, et al. Crossed cerebellar diaschisis after stroke: can perfusion-weighted mri show functional inactivation? *J Cereb Blood Flow Metab* 2011; 31: 1493–1500.
29. Kamouchi M, Fujishima M, Saku Y, et al. Crossed cerebellar hypoperfusion in hyperacute ischemic stroke. *J Neurol Sci* 2004; 225: 65–69.
30. Schmahmann JD. Vascular syndromes of the thalamus. *Stroke* 2003; 34: 2264–2278.
31. Carmichael ST, Tatsukawa K, Katsman D, et al. Evolution of diaschisis in a focal stroke model. *Stroke* 2004; 35: 758–763.
32. Kim D, Kim RG, Kim HS, et al. Longitudinal changes in resting-state brain activity in a capsular infarct model. *J Cereb Blood Flow Metab* 2015; 35: 882.
33. Shishido F, Uemura K, Inugami A, et al. Remote effects in MCA territory ischemic infarction: a study of regional cerebral blood flow and oxygen metabolism using positron computed tomography and 15o labeled gases. *Radiat Med* 1987; 5: 36–41.
34. De Reuck J, Decoo D, Lemahieu I, et al. Ipsilateral thalamic diaschisis after middle cerebral artery infarction. *J Neurol Sci* 1995; 134: 130–135.
35. Ahn HS and Kim KK. Two cases of crossed cerebellar diaschisis with or without thalamic lesion on brain mri in status epilepticus. *J Epilepsy Res* 2014; 4: 74–77.
36. Graffeo CS, Snyder KA, Nasr DM, et al. Prognostic and mechanistic factors characterizing seizure-associated crossed cerebellar diaschisis. *Neurocritical Care*. Epub ahead of print 11 June 2015. DOI: 10.1007/s12028-015-0155-4.
37. Tecco JM, Wuilmart P, Lasseaux L, et al. Cerebello-thalamo-cerebral diaschisis: a case report. *J Neuroimaging* 1998; 8: 115–116.

38. Cicirata F, Zappala A, Serapide MF, et al. Different pontine projections to the two sides of the cerebellum. *Brain Res Brain Res Rev* 2005; 49: 280–294.
39. Kultas-Ilinsky K, Ilinsky IA and Verney C. Glutamic acid decarboxylase isoform 65 immunoreactivity in the motor thalamus of humans and monkeys: gamma-aminobutyric acidergic connections and nuclear delineations. *J Comp Neurol* 2011; 519: 2811–2837.
40. Yamauchi H, Fukuyama H and Kimura J. Hemodynamic and metabolic changes in crossed cerebellar hypoperfusion. *Stroke* 1992; 23: 855–860.
41. Ito H, Kanno I, Shimosegawa E, et al. Hemodynamic changes during neural deactivation in human brain: a positron emission tomography study of crossed cerebellar diaschisis. *Ann Nucl Med* 2002; 16: 249–254.
42. Otte A, Roelcke U, von Ammon K, et al. Crossed cerebellar diaschisis and brain tumor biochemistry studied with positron emission tomography, [¹⁸F]fluorodeoxyglucose and [¹¹C]methionine. *J Neurol Sci* 1998; 156: 73–77.
43. Lim JS, Ryu YH, Kim BM, et al. Crossed cerebellar diaschisis due to intracranial hematoma in basal ganglia or thalamus. *J. Nucl Med* 1998; 39: 2044–2047.
44. Pantano P, Baron JC, Samson Y, et al. Crossed cerebellar diaschisis. *Further studies*. *Brain* 1986; 109 (Pt 4): 677–694.
45. Feeney DM and Baron JC. Diaschisis. *Stroke* 1986; 17: 817–830.
46. Strick PL, Dum RP and Fiez JA. Cerebellum and non-motor function. *Annu Rev Neurosci* 2009; 32: 413–434.
47. Barbas H, Garcia-Cabezas MA and Zikopoulos B. Frontal-thalamic circuits associated with language. *Brain Lang* 2013; 126: 49–61.
48. Binkofski F and Buccino G. The role of ventral premotor cortex in action execution and action understanding. *J Physiol Paris* 2006; 99: 396–405.
49. Chen SH and Desmond JE. Temporal dynamics of cerebro-cerebellar network recruitment during a cognitive task. *Neuropsychologia* 2005; 43: 1227–1237.
50. Takasawa M, Watanabe M, Yamamoto S, et al. Prognostic value of subacute crossed cerebellar diaschisis: single-photon emission ct study in patients with middle cerebral artery territory infarct. *AJNR Am J Neuroradiol* 2002; 23: 189–193.
51. Chakravarty A. MR evaluation of crossed and uncrossed cerebral-cerebellar diaschisis. *Acta Neurol Scand* 2003; 108: 60–65.
52. Yamada H, Koshimoto Y, Sadato N, et al. Crossed cerebellar diaschisis: assessment with dynamic susceptibility contrast MR imaging. *Radiology* 1999; 210: 558–562.

V.3 Early CT perfusion mismatch in acute stroke is not time-dependent but relies on collateralization grade

Louisa von Baumgarten, Kolja M. Thierfelder, Sebastian E. Beyer, Alena B. Baumann, **Christine Bollwein**, Hendrik Janssen, Maximilian F. Reiser, Andreas Straube, Wieland H. Sommer

Neuroradiology. 2016 Apr; 58(4):357-65

Impact factor 2016: 2,3

Early CT perfusion mismatch in acute stroke is not time-dependent but relies on collateralization grade

Louisa von Baumgarten¹ · Kolja M. Thierfelder² · Sebastian E. Beyer² · Alena B. Baumann² · Christine Bollwein² · Hendrik Janssen³ · Maximilian F. Reiser² · Andreas Straube¹ · Wieland H. Sommer²

Received: 3 December 2015 / Accepted: 6 January 2016 / Published online: 18 January 2016
© Springer-Verlag Berlin Heidelberg 2016

Abstract

Introduction Factors that determine the extent of the penumbra in the initial diagnostic workup using whole brain CT Perfusion (WB-CTP) remain unclear. The purpose of the current study was to determine a possible dependency of the initial mismatch size between cerebral blood flow (CBF) and cerebral blood volume (CBV) from time after symptom onset, leptomeningeal collateralization, and occlusion localization in acute middle cerebral artery (MCA) infarctions.

Methods Out of an existing cohort of 992 consecutive patients receiving multiparametric CT scans including WB-CTP due to suspected stroke, we included patients who had (1) a witnessed time of symptom onset, (2) an infarction of the MCA territory as documented by follow-up imaging, and (3) an initial CBF volume of >10 ml. CBF and CBV lesion sizes, collateralization grade, and the site of occlusion were determined.

Results We included 103 patients. Univariate analysis showed that time from symptom onset (168 ± 91.2 min) did not correlate with relative or absolute mismatch volumes ($p=0.458$ and $p=0.921$). Higher collateralization gradings were

associated with small absolute mismatch volumes ($p=0.004$ and $p<0.001$). Internal carotid artery (ICA) occlusions were associated with large absolute mismatch volumes ($p=0.004$). Multivariate analysis confirmed that ICA occlusion was associated with large absolute mismatch volumes ($p=0.005$), and high collateral grade was associated with small absolute mismatch volumes ($p=0.017$).

Conclusions There is no significant correlation between initial CTP mismatch and time after symptom onset. Predictors of mismatch size include the extent of the collaterals and a proximal location of the occlusion.

Keywords CT perfusion · Leptomeningeal collateralization · Acute ischemic stroke · Penumbra imaging · Flow-volume mismatch

Introduction

Immediately after the onset of ischemia, the infarct core is thought to be surrounded by a hypoperfused but potentially salvageable ischemic penumbra. Without reperfusion, the infarct core expands into the hypoperfused tissue of the penumbra. It has been proposed that the rate of this expansion is proportional to the susceptibility of the underlying tissue to ischemia, the severity of the hypoperfusion, and the time elapsed after stroke onset [1]. With prompt reperfusion, penumbra tissue salvage may be linked to improved clinical outcomes [2].

The current recommendations for stroke recanalization are limited to a small window of time elapsed after symptom onset. It is commonly assumed that in the absence of reperfusion, the expansion of the infarct core occurs fast [3] and that treatment efficacy therefore rapidly decreases with time [4–6]. Currently, the time window approved for using intravenous

LvB and KMT contributed equally to this work.

✉ Louisa von Baumgarten
Louisa.vonBaumgarten@med.uni-muenchen.de

¹ Department of Neurology, University of Munich Hospitals, Grosshadern Campus, Marchioninstr. 15, 81377 Munich, Germany

² Institute for Clinical Radiology, Ludwig-Maximilians-University Hospital Munich, Munich, Germany

³ Department of Neuroradiology, Ludwig-Maximilians-University Hospital Munich, Munich, Germany

tissue-type plasminogen activator is limited to 4.5 h after symptom onset [7], and as a consequence of the narrow time window systemic thrombolysis rates among patients with acute stroke have been reported to range among 5 % [8, 9] and, more recently, up to 13.9 % [10].

In recent years, there was an increase in the rate of computed tomography angiography (CTA) and computed tomography perfusion (CTP) studies in the setting of acute ischemic stroke, and both techniques were associated with increased use of reperfusion therapy [11]. The idea of CTP is to discriminate areas of potentially salvageable penumbra from the ischemic core by analyzing perfusion parameter maps. Most commonly, the mismatch is calculated between cerebral blood flow (CBF) and cerebral blood volume (CBV) or between mean transit time (MTT) maps and CBV [12–14].

While earlier generation CT-scanners only allowed examination of perfusion in two selected axial slices precluding evaluation of a complete volumetric perfusion status [15], newer CT-scanners now enable whole-brain acquisition allowing assessment of the total volume of the ischemic region and the tissue at risk [16, 17]. Studies using whole-brain penumbral imaging might have the potential to personalize treatment strategies in individual patients independent of the time window [2, 18]. Patient enrollment into clinical trials increasingly considers the extent of the ischemic penumbra rather than the time elapsed after symptom onset [19, 20], although there is an ongoing and controversial debate on the value of the imaging selection hypothesis [21].

However, the factors that determine the extent of the penumbra in the initial diagnostic workup using whole brain CTP remain unclear. Therefore, the purpose of the current study was to determine the dependency of the initial mismatch size between CBF and CBV with respect to time after symptom onset, leptomeningeal collateralization, and occlusion localization in patients with acute ischemic stroke of the media territory.

Materials and methods

Study design and study population

The institutional review board approved the study and waived requirement for informed consent. Our initial cohort consisted of 992 consecutive patients admitted to our institution undergoing multiparametric CT including WB-CTP due to suspected stroke between April 2009 and June 2012. We retrospectively included all patients with the following:

1. A CT perfusion deficit suggestive of acute cerebral infarction
2. A documented time of witnessed symptom onset

3. A confirmed ischemic infarction in the MCA territory on follow-up MRI within 72 h after the initial CT scan

We excluded patients with the following:

2. A multiparametric CT scan with non-diagnostic quality of non-enhanced CT (NECT), CT angiography, or CT perfusion
2. A CBF lesion size of less than 10 ml, since mismatch calculations below this threshold may be strongly affected by small variances in lesion volumetry

Time from symptom onset was defined as the time interval between symptom onset and CT perfusion imaging. Data concerning the time of symptom onset were collected by review of the medical chart and were only included into the analyses in case of a documented time point of witnessed symptom onset.

CT examination protocol

The multiparametric CT protocol consisted of NECT to exclude intracranial hemorrhage, a supraaortic CTA, and WB-CTP, all performed using one of the following CT-scanners: SOMATOM Definition AS+, a 128 slice CT scanner; SOMATOM Definition Flash, a 128 slice dual source CT scanner; and SOMATOM Definition Edge, a 128 slice CT scanner (all by Siemens Healthcare, Erlangen, Germany).

WB-CTP images were obtained with a collimation of 0.6 mm and a scan coverage of 100 mm in the z-axis using adaptive spiral scanning. One scan was acquired every 1.5 s. Tube voltage was 80 kV and tube current was 200 mAs. Computed tomography dose index ($CTDI_{vol}$) was 276 mGY. A volume of 35 mL of highly iodinated contrast agent was administered at a flow rate of 5 mL/s followed by a saline flush of 40 mL at 5 mL/s. Injections of contrast agent were performed through an 18-gauge needle (18G × 1 3/4, Braun, Melsungen, Germany) placed in the cubital vein. Thirty-one axial slices were reconstructed per view with a thickness of 10 mm and an increment of 3 mm.

CT-perfusion image processing and analysis

CT perfusion was used to assess the absolute and the relative mismatch between CBV and CBF. Relative mismatch was defined as the percentage of the CBF perfusion deficit without corresponding CBV lesion. Absolute mismatch was defined as CBF perfusion deficit – CBV lesion volume.

The axial CTP images were transferred to a workstation (Syngo MMWP, VA21A; Siemens Healthcare, Erlangen, Germany), and perfusion analysis was performed with the software provided by the vendor, Syngo Volume Perfusion CT Neuro (Version VA21A, Siemens Healthcare, Erlangen,

Germany), using a semiautomated deconvolution algorithm (Auto Stroke MTT). OsiriX version 4.0 imaging software (<http://www.osirix-viewer.com>) was used for offline 3D assessment of CBV and CBF lesion size as previously described [17]. Briefly, we manually segmented the perfusion deficit on every axial slice using the OsiriX closed polygon tool to create a region of interest. The perfusion deficit volume was calculated using the OsiriX volume calculation tool. All volumetric analyses were performed by a reader of CT perfusions with 3 years of experience in stroke imaging, blinded to clinical information and follow-up scans.

CT angiography image analysis

CT angiography was used to determine the location of the vessel occlusion. Furthermore, leptomeningeal collaterals were assessed on baseline CTA by use of the regional leptomeningeal collateralization score (rLMC), a previously published ordinal scoring system that is based on the Alberta Stroke Program Early CT Score (ASPECTS) template and which has been shown to have excellent inter-rater reliability [22–24]. Briefly, the score is based on scoring pial and lenticulostriate arteries (0 no, 1 less, and 2 equal or more prominent compared with matching region in opposite hemisphere in six aspect regions (M1–M6) plus anterior cerebral artery region and basal ganglia. Pial arteries in the Sylvian sulcus are double-weighted). Collateral status by use of the rLMC score (0–20) was trichotomized into three grades—1 poor (0–10), 2 intermediate (11–16), and 3 good (17–20)—according to previously published literature [22–24]. Two readers, one with 8 years and one with 2 years of experience

in stroke imaging, independently reviewed and scored by consensus baseline CT scans and CTA. Both readers were blinded to clinical information and follow-up scans. In case of disagreement, a consensus was reached in a separate session.

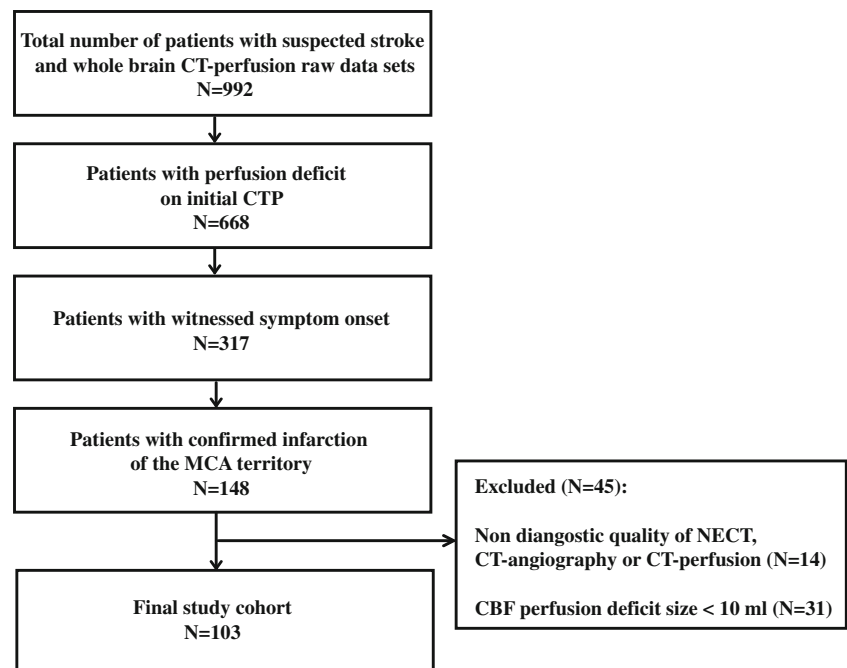
Follow-up imaging

The MRI follow-up examination comprised a T2* sequence, a fluid-attenuated inversion recovery (FLAIR) sequence, a diffusion-weighted imaging (DWI) sequence, and a time-of-flight (TOF)-MR angiography.

Statistical analysis

We performed all statistical analyses using SPSS (Version 21.0; IBM, Armonk, NY). All metric and normally distributed variables are reported as mean \pm standard deviation; non-normally distributed variables are presented as median and interquartile ranges. Categorical variables are presented as frequency and percentage. Normal distribution was assessed using the Kolmogorov-Smirnov test. In case of not-normally distributed variables, a square root transformation was performed and the Kolmogorov-Smirnov test was repeated. Univariate linear regression analysis was used to test the association between predictors and outcome variables. The following variables were included as predictors: age, sex, time from symptom onset, and location of occlusion (internal carotid artery, M1 segment of MCA, M2 segment of MCA, other occlusion, no occlusion, and collateral grade (as ordinal variable as previously practiced)). Multivariate linear regression was used for adjusted analyses. Variables significantly

Fig. 1 Inclusion and exclusion flow chart



associated with a favorable outcome ($p < 0.2$) in the univariate regression were included in the multivariate models. P values below 0.05 were considered to indicate statistical significance. To provide interpretable results in the multivariate analysis in cases of not-normally distributed variables and square root transformation, analyses were performed for the original variables and the square root transformed variables.

Results

Study population

Among our initial cohort of 992 patients, 698 had an initial CT perfusion alteration suggestive of an acute infarction. Of those, 317 had a documented time of witnessed symptom onset. Out of this subgroup, a total of 148 patients had MRI follow-up imaging documenting an ischemic lesion in the corresponding MCA territory and were included into further analysis. We excluded 31 patients due to an initial CBF lesion size of < 10 ml, 14 due to non-diagnostic quality of NECT, CTA, or CT perfusion. The remaining 103 patients constituted the final study cohort (Fig. 1).

Table 1 Patient Characteristics

	All patients ($N = 103$)
Age—year ^a	70.2 ± 14.3
Male sex—no. (%)	58 (56.3)
Time from symptom onset—min ^a	168.5 ± 91.2
CBF lesion size—ml ^b	128.0 (57.4–194.8)
CBV lesion size—ml ^b	40.4 (10.8–70.4)
Relative mismatch—% ^b	63.5 (49.8–78.7)
Absolute mismatch—ml ^b	68.7 (30.7–109.8)
Vessel occlusion	
ICA—no. (%)	29 (28.2)
M1—no. (%)	49 (47.6)
M2—no. (%)	27 (26.2)
Other—no. (%)	8 (7.8)
None—no. (%)	15 (14.6)
Collateralization	
Grade 1 (poor, rLMC 0–10)	46 (44.7)
Grade 2 (intermediate, rLMC 11–16)	34 (33.0)
Grade 3 (good, rLMC 17–20)	23 (22.3)
ASPECTS ^a	8.11 ± 2.71

ASPECTS Alberta Stroke Programme Early CT Score, ICA Internal Carotid Artery, rLMC score regional leptomeningeal collateralization score

^a Mean ± SD

^b Median (IQR)

Baseline characteristics

In total, 103 patients with a mean age of 72 ± 14 years were analyzed including 58 men and 45 women. An occlusion of the M1 segment of the MCA was detected in 49 (47.6 %) patients. Internal carotid artery (ICA) occlusions were diagnosed in 29 (28.2 %) and M2 segment occlusions in 27 (25.2 %) patients, respectively. Eight patients (7.8 %) had occlusions other than ICA and M1 or M2 segments. No occlusion could be detected in 15 (14.6 %) patients. Twenty-two (16.9 %) patients had more than one occlusion. Median relative mismatch was 63.5 % (range 49.8–78.7 %), median absolute mismatch volume was 68.7 ml (range 30.7–109.8 ml), and mean time from symptom onset was 168.5 ± 91.2 min. Collaterals were graded by use of the cLMC score as 1 (poor, rLMC 0–10) in 46 patients (44.7 %), as 2 (intermediate, rLMC 11–16) in 34 patients (33.0 %), and as 3 (good, rLMC 17–20) in 23 patients (22.3 %). Patient characteristics are summarized in Table 1.

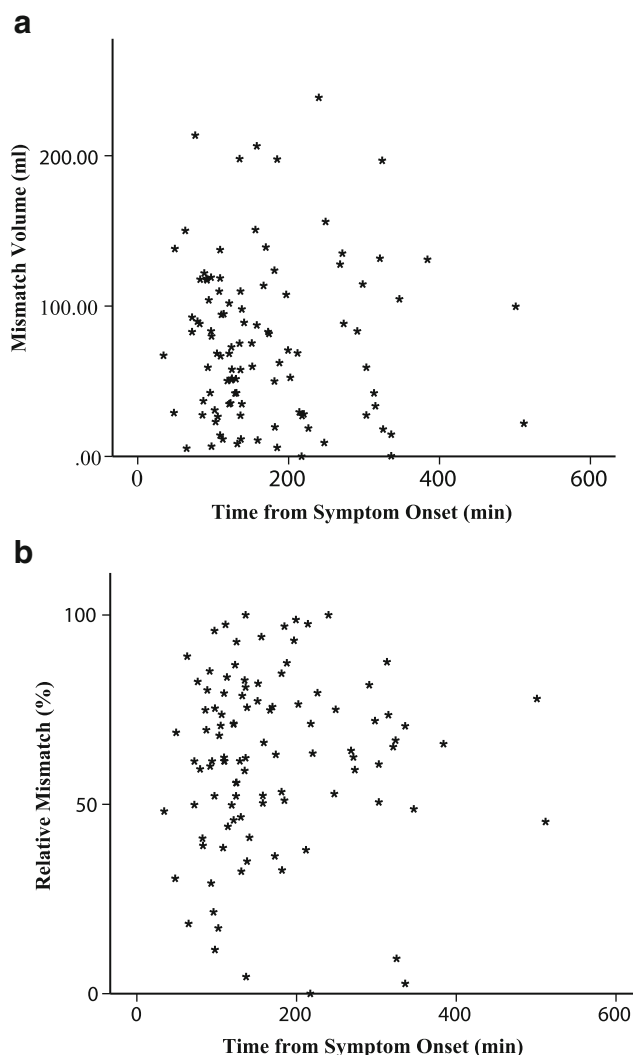


Fig. 2 a Absolute and b relative CT perfusion mismatch versus time from symptom onset

Factors associated with the extent of relative and absolute mismatch volume

The relative and the absolute mismatch volumes with respect to the time elapsed after symptom onset for all 103 patients are illustrated in Fig. 2. There was no apparent correlation between absolute or relative mismatch and time from symptom onset. The results of the univariate analysis testing for correlations between time from symptom onset, leptomeningeal collateralization, or occlusion location on one hand and relative or absolute CT perfusion mismatch volumes on the other hand are shown in Table 2. Time from symptom onset was not significantly associated with either relative or with absolute mismatch volume ($p=0.458$ and $p=0.921$, respectively), neither could a trend be observed in our data. Intermediate collateralization grade, however, was significantly associated with the relative ($p=0.010$) and, inversely, with the absolute mismatch volume ($p=0.004$), indicating e.g. a comparatively small infarct core and a small absolute penumbra. Likewise, good collateralization was associated with a small absolute mismatch volume ($p<0.001$). The correlation between collateralization grade and absolute mismatch volumes is represented in Fig. 3. The association with the relative mismatch, however, was not significant ($p=0.112$), most probably due to the heterogeneity of the occlusion sites.

No significant correlation was seen between the localization of the occlusion and mismatch volumes with the exception of ICA occlusion, which was associated with a large absolute (but not relative) mismatch volume ($p=0.004$).

Similar results were obtained in the multivariate analysis: Good collateralization grade proved to be significantly associated with a small absolute mismatch volume ($p=0.017$) and

ICA occlusion was associated with a large absolute mismatch volume ($p=0.005$). Time from symptom onset was not normally distributed. Consistency of the results was confirmed after square root transformation of this variable.

Subgroup analysis

To rule out a major influence of the occlusion site heterogeneity, a subgroup analysis was performed for all patients with a proximal (M1 or M2) MCA occlusion ($n=75$). The results of the univariate analysis are given in Table 3. Consistent with the entire group, there was no correlation between time from symptom onset and relative ($p=0.781$) as well as absolute mismatch volume (0.908). Only the collateralization grade was significantly associated with relative mismatch (intermediate collateralization, $p=0.007$, good collateralization $p=0.007$) and absolute mismatch volume ($p=0.007$ and $p=0.039$, respectively).

Discussion

In our study on factors that influence the extent of the early CT perfusion mismatch, we could show a lack of correlation between the initial CTP mismatch and time from symptom onset. Predictive factors for mismatch size were the status of leptomeningeal collateralization as well as the presence of a proximal occlusion localization.

Our data support and further extend prior reports that did not find a correlation between time from symptom onset and penumbral volume.

Table 2 Univariate linear regression analysis for relative and absolute CT perfusion mismatch

	Relative mismatch (%)	Absolute mismatch (ml)
Age	$\beta = -0.100; p = 0.536$	$\beta = -0.271; p = 0.463$
Male sex	$\beta = 4.575; p = 0.280$	$\beta = -13.272; p = 0.206$
Time from symptom onset	$\beta = 3.302; p = 0.458$	$\beta = -0.006; p = 0.921$
Vessel occlusion		
ICA	$\beta = -4.875; p = 0.475$	$\beta = 32.238; p = 0.004$
M1	$\beta = -2.894; p = 0.637$	$\beta = 23.428; p = 0.060$
M2	$\beta = 0.781; p = 0.907$	$\beta = -1.483; p = 0.912$
Other	$\beta = -5.683; p = 0.560$	$\beta = -36.974; p = 0.061$
None	Reference	Reference
Collateralization (rLMC score)		
Grade 1 (poor, rLMC 0–10)	Reference	Reference
Grade 2 (intermediate, rLMC 11–16)	$\beta = 13.274; p = 0.010$	$\beta = -32.171; p = 0.004$
Grade 3 (good, rLMC 17–20)	$\beta = 9.200; p = 0.112$	$\beta = -52.533; p < 0.001$

ICA internal carotid artery, rLMC score regional leptomeningeal collateralization score

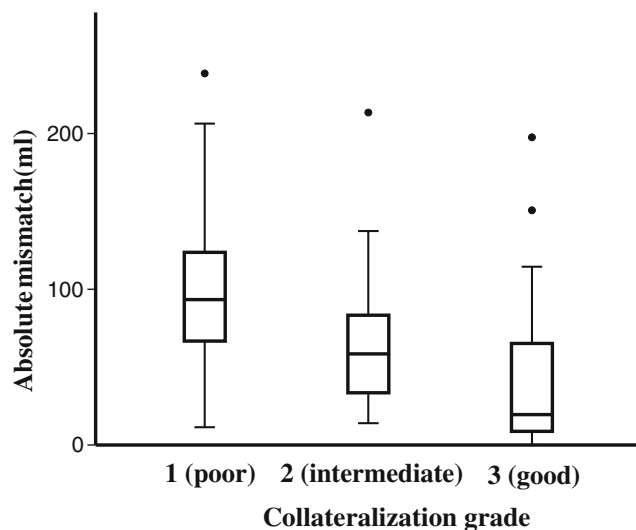


Fig. 3 Correlation between collateralization grade and absolute mismatch volume. Data represent median and interquartile range; *black dots* represent outliers

Time dependency of the penumbral volume was so far mainly addressed using MRI techniques. It was shown that within the first 6 h after stroke onset, there were no significant time-dependent differences in degree and volume of perfusion and diffusion impairment mismatch (PWI/DWI mismatch) [25]. In another study that included 109 consecutive acute anterior circulation stroke patients, Copen et al. demonstrated that a substantial percentage of stroke patients continue to demonstrate a PWI/DWI mismatch beyond 9 h up to 24 h after symptom onset. According to this study, the existence of a mismatch beyond 9 h was more likely in patients with than in patients without a proximal arterial occlusion [26]. Other studies involving smaller cohorts reported similar results

[27–30]. In a study including 186 patients with major anterior circulation ischemic strokes, it was shown that there is a poor correlation between infarct volume and time after stroke onset and there is an unexpected wide range of individual infarct growth rates [31]. Hence, using MRI-based penumbral imaging, the time elapsed after symptom onset is only a poor predictor of penumbral volume.

Penumbral imaging using CTP provides similar information as MR imaging [32, 33]. In a CTP study conducted to determine whether optimal CTP thresholds for ischemic core and penumbra are time-dependent, the authors report no changes in the threshold within the first 15 h after symptom onset. In fact, selected patients presenting even 24 h after stroke onset had varying areas of penumbra and there was no correlation between the ratio of penumbra to ischemic core and the time elapsed from symptom onset on CTP [34]. Another study also failed to find a correlation between CTP mismatch, defined as a CTP ASPECT mismatch of ≥ 2 between CBV and MTT, and the time from symptom onset [35]. However, the variable and limited CTP coverage of both studies (20 mm [35] and 20–80 mm [34]) precludes translating the observed phenomena to scanners with more extensive brain coverage. Our results, therefore, for the first time confirm that there is no correlation between time from symptom onset and CTP mismatch as assessed by whole brain CTP.

The absence of a correlation between time from symptom onset and a shrinking penumbra as well as the maintenance of a large mismatch in patients for a relatively long time might be explained by a large variability in the cerebral perfusion via the collateral circulation. Indeed, our results show that the extent of the CTP mismatch is strongly correlated with the degree of leptomeningeal collateralization. In line with our findings, it was shown that the quality of collateral blood flow

Table 3 Subgroup analysis: univariate linear regression analysis for relative and absolute CT perfusion mismatch in proximal MCA occlusions ($n = 76$)

	Relative mismatch (%)	Absolute mismatch (ml)
Age—year	$\beta = -0.087; p = 0.647$	$\beta = -0.032; p = 0.935$
Male sex	$\beta = -5.077; p = 0.336$	$\beta = 5.047; p = 0.645$
Time from symptom onset	$\beta = 0.008; p = 0.781$	$\beta = -0.007; p = 0.908$
Vessel occlusion		
M1	$\beta = 6.652; p = 0.778$	$\beta = 73.130; p = 0.116$
M2	$\beta = 7.774; p = 0.736$	$\beta = 38.633; p = 0.392$
None	Reference	Reference
Collateralization (rLMC score)		
Grade 1 (poor, rLMC 0–10)	Reference	Reference
Grade 2 (intermediate, rLMC 11–16)	$\beta = 14.538; p = 0.007$	$\beta = -30.987; p = 0.007$
Grade 3 (good, rLMC 17–20)	$\beta = 22.723; p = 0.007$	$\beta = -17.875; p = 0.039$

MCA middle cerebral artery, ICA internal carotid artery, rLMC score regional leptomeningeal collateralization score

and the degree of PWI/DWI mismatch are strongly related, and both are associated with infarct growth [36]. The impact of collaterals has been addressed in several other studies, and good collaterals are considered to protect the penumbra and to predict stable mismatch [30, 37–39]. In line with previous studies, we can show that a higher collateralization degree is associated with a high relative mismatch but small absolute penumbral volume [40], indicating e.g. a comparatively small infarct core and a small absolute penumbra. Furthermore, pretreatment collateral status was proven to have prognostic relevance for the final infarct size and the outcome of patients with ischemic stroke [23, 40–43]. For example, Jung et al. could show that the quality of collaterals and the quantity of reperfusion, but not the time from symptom onset, were the major factors determining the penumbra loss as assessed by serial PWI/DWI imaging in patients with proximal middle cerebral artery occlusions [44]. Similarly, Menon et al. included 138 patients (MCA/M1 and/or intracranial occlusion) in a retrospective single-center study and demonstrated that a good leptomeningeal collateralization correlates strongly with the size of infarct core at baseline and is a strong independent predictor of final infarct size and clinical outcome. Serial imaging revealed that progressive collateral failure in a period of up to 5 days is associated with infarct growth [22].

There are limitations to this study, which need to be taken into account when interpreting the data. Firstly, as in any retrospective study, there is the risk of a selection bias. All enrolled patients, however, were recruited from the prospectively collected stroke registry, and standardized stroke protocols were applied to minimize this bias. Secondly, inherent limitations of the methodology of CTP should be considered. We assessed the extension of the perfusion deficit in comparison to the contralateral side, thereby using a relative approach as previously described [17]. However, we avoided using rigid quantitative perfusion thresholds for the definition of the ischemic core since post-processing methods vary widely among manufacturers [45] and since there are currently no operationally defined and universally accepted thresholds [46].

We considered other potential confounders; one possibility was the heterogeneity in occlusion sites. However, the same lack of correlation between time from symptom onset and CTP mismatch persisted when we evaluated patients with proximal occlusion of the MCA only (M1 and M2 occlusions). Furthermore, we could not include information on the etiology of the vessel occlusion (thrombosis vs. embolism) although this might be relevant for the resulting perfusion deficit.

Finally, our conclusions are only valid for infarctions of the media territory and a time from symptom onset with up to 8 h, with the majority within the conventional time window of 4.5 h. We do not know whether similar conclusions can be

drawn for patients with occlusions of other cerebral vessels and after more than 8 h after symptom onset.

Conclusion

Our study emphasizes the importance of the extent of collateralization rather than time from symptom onset as a critical factor in determining CTP mismatch after acute ischemic stroke. The missing correlation between mismatch and time from symptom onset supports the current paradigm shift from “time is brain” to “physiology is brain.” The strong correlation between collateralization grade and penumbral volume supports this concept and encourages further research in this field.

Compliance with ethical standards We declare that all human and animal studies have been approved by the institutional Ethics Committee of the Medical Faculty of the Ludwigs-Maximilians University Munich and have therefore been performed in accordance with the ethical standards laid down in the 1964 declaration of Helsinki and its later amendments. We declare that the Ethics Committee waived informed patient consent.

Conflict of interest We declare that we have no conflict of interest.

References

1. Jones TH, Morawetz RB, Crowell RM, Marcoux FW, FitzGibbon SJ, DeGirolami U, Ojemann RG (1981) Thresholds of focal cerebral ischemia in awake monkeys. *J Neurosurg* 54(6):773–782. doi:10.3171/jns.1981.54.6.0773
2. Abou-Chebl A (2010) Endovascular treatment of acute ischemic stroke may be safely performed with no time window limit in appropriately selected patients. *Stroke* 41(9):1996–2000. doi:10.1161/STROKEAHA.110.578997
3. Saver JL (2006) Time is brain—quantified. *Stroke* 37(1):263–266. doi:10.1161/01.STR.0000196957.55928.ab
4. Khatri P, Abruzzo T, Yeatts SD, Nichols C, Broderick JP, Tomsick TA, Ims I, Investigators II (2009) Good clinical outcome after ischemic stroke with successful revascularization is time-dependent. *Neurology* 73(13):1066–1072. doi:10.1212/WNL.0b013e3181b9c847
5. Hacke W, Kaste M, Fieschi C, von Kummer R, Davalos A, Meier D, Larrue V, Bluhmki E, Davis S, Donnan G, Schneider D, Diez-Tejedor E, Trouillas P (1998) Randomised double-blind placebo-controlled trial of thrombolytic therapy with intravenous alteplase in acute ischaemic stroke (ECASS II). Second European-Australasian acute stroke study investigators. *Lancet* 352(9136):1245–1251
6. Emberson J, Lees KR, Lyden P, Blackwell L, Albers G, Bluhmki E, Brott T, Cohen G, Davis S, Donnan G, Grotta J, Howard G, Kaste M, Koga M, von Kummer R, Lansberg M, Lindley RI, Murray G, Olivot JM, Parsons M, Tilley B, Toni D, Toyoda K, Wahlgren N, Wardlaw J, Whiteley W, Del Zoppo GJ, Baigent C, Sandercock P, Hacke W, for the Stroke Thrombolysis Trialists' Collaborative G, (2014) Effect of treatment delay, age, and stroke severity on the

- effects of intravenous thrombolysis with alteplase for acute ischaemic stroke: a meta-analysis of individual patient data from randomised trials. *Lancet*. doi:10.1016/S0140-6736(14)60584-5
7. Jauch EC, Saver JL, Adams HP Jr, Bruno A, Connors JJ, Demaerschalk BM, Khatri P, McMullan PW Jr, Qureshi AI, Rosenfield K, Scott PA, Summers DR, Wang DZ, Wintermark M, Yonas H, American Heart Association Stroke C, Council on Cardiovascular N, Council on Peripheral Vascular D, Council on Clinical C (2013) Guidelines for the early management of patients with acute ischemic stroke: a guideline for healthcare professionals from the American Heart Association/American Stroke Association. *Stroke* 44(3):870–947. doi:10.1161/STR.0b013e318284056a
 8. Adeoye O, Hornung R, Khatri P, Kleindorfer D (2011) Recombinant tissue-type plasminogen activator use for ischemic stroke in the United States: a doubling of treatment rates over the course of 5 years. *Stroke* 42(7):1952–1955. doi:10.1161/STROKEAHA.110.612358
 9. de Los Rios la Rosa F, Khoury J, Kissela BM, Flaherty ML, Alwell K, Moomaw CJ, Khatri P, Adeoye O, Woo D, Ferioli S, Kleindorfer DO (2012) Eligibility for intravenous recombinant tissue-type plasminogen activator within a population: the effect of the European Cooperative acute stroke study (ECASS) III trial. *Stroke* 43(6):1591–1595. doi:10.1161/STROKEAHA.111.645986
 10. Asplund K, Sukhova M, Wester P, Stegmayr B (2015) Diagnostic procedures, treatments, and outcomes in stroke patients admitted to different types of hospitals. *Stroke* 46(3):806–812. doi:10.1161/STROKEAHA.114.007212
 11. Vagal A, Meganathan K, Kleindorfer DO, Adeoye O, Hornung R, Khatri P (2014) Increasing use of computed tomographic perfusion and computed tomographic angiograms in acute ischemic stroke from 2006 to 2010. *Stroke* 45(4):1029–1034. doi:10.1161/STROKEAHA.113.004332
 12. Wintermark M, Flanders AE, Velthuis B, Meuli R, van Leeuwen M, Goldsher D, Pineda C, Serena J, van der Schaaf I, Waaijer A, Anderson J, Nesbit G, Gabriely I, Medina V, Quiles A, Pohlman S, Quist M, Schnyder P, Bogousslavsky J, Dillon WP, Pedraza S (2006) Perfusion-CT assessment of infarct core and penumbra: receiver operating characteristic curve analysis in 130 patients suspected of acute hemispheric stroke. *Stroke* 37(4):979–985. doi:10.1161/01.STR.0000209238.61459.39
 13. Campbell BC, Purushotham A, Christensen S, Desmond PM, Nagakane Y, Parsons MW, Lansberg MG, Mlynash M, Straka M, De Silva DA, Olivot JM, Bammer R, Albers GW, Donnan GA, Davis SM (2012) The infarct core is well represented by the acute diffusion lesion: sustained reversal is infrequent. *J Cereb Blood Flow Metab* 32(1):50–56. doi:10.1038/jcbfm.2011.102
 14. De Silva DA, Churilov L, Olivot JM, Christensen S, Lansberg MG, Mlynash M, Campbell BC, Desmond P, Straka M, Bammer R, Albers GW, Davis SM, Donnan GA (2011) Greater effect of stroke thrombolysis in the presence of arterial obstruction. *Ann Neurol* 70(4):601–605. doi:10.1002/ana.22444
 15. Schaefer PW, Barak ER, Kamalian S, Gharai LR, Schwamm L, Gonzalez RG, Lev MH (2008) Quantitative assessment of core/penumbra mismatch in acute stroke: CT and MR perfusion imaging are strongly correlated when sufficient brain volume is imaged. *Stroke* 39(11):2986–2992. doi:10.1161/STROKEAHA.107.513358
 16. Murayama K, Katada K, Nakane M, Toyama H, Anno H, Hayakawa M, Ruiz DS, Murphy KJ (2009) Whole-brain perfusion CT performed with a prototype 256-detector row CT system: initial experience. *Radiology* 250(1):202–211. doi:10.1148/radiol.2501071809
 17. Thierfelder KM, Sommer WH, Baumann AB, Klotz E, Meinel FG, Strobl FF, Nikolaou K, Reiser MF, von Baumgarten L (2013) Whole-brain CT perfusion: reliability and reproducibility of volumetric perfusion deficit assessment in patients with acute ischemic stroke. *Neuroradiology* 55(7):827–835. doi:10.1007/s00234-013-1179-0
 18. Abou-Chebl A, Lin R, Hussain MS, Jovin TG, Levy EI, Liebeskind DS, Yoo AJ, Hsu DP, Rymer MM, Tayal AH, Zaidat OO, Natarajan SK, Nogueira RG, Nanda A, Tian M, Hao Q, Kalia JS, Nguyen TN, Chen M, Gupta R (2010) Conscious sedation versus general anesthesia during endovascular therapy for acute anterior circulation stroke: preliminary results from a retrospective, multicenter study. *Stroke* 41(6):1175–1179. doi:10.1161/STROKEAHA.109.574129
 19. Almekhlafi MA, Demchuk AM, Mishra S, Bal S, Menon BK, Wiebe S, Clement FM, Wong JH, Hill MD, Goyal M (2013) Malignant emboli on transcranial Doppler during carotid stenting predict postprocedure diffusion-weighted imaging lesions. *Stroke* 44(5):1317–1322. doi:10.1161/STROKEAHA.111.000659
 20. Broderick JP, Palesch YY, Demchuk AM, Yeatts SD, Khatri P, Hill MD, Jauch EC, Jovin TG, Yan B, Silver FL, von Kummer R, Molina CA, Demaerschalk BM, Budzik R, Clark WM, Zaidat OO, Malisch TW, Goyal M, Schonewille WJ, Mazighi M, Engelter ST, Anderson C, Spilker J, Carrozzella J, Ryckborst KJ, Janis LS, Martin RH, Foster LD, Tomsick TA (2013) Endovascular therapy after intravenous t-PA versus t-PA alone for stroke. *N Engl J Med* 368(10):893–903. doi:10.1056/NEJMoa1214300
 21. Kidwell CS, Jahan R, Gornbein J, Alger JR, Nenov V, Ajani Z, Feng L, Meyer BC, Olson S, Schwamm LH, Yoo AJ, Marshall RS, Meyers PM, Yavagal DR, Wintermark M, Guzy J, Starkman S, Saver JL, Investigators MR (2013) A trial of imaging selection and endovascular treatment for ischemic stroke. *N Engl J Med* 368(10):914–923. doi:10.1056/NEJMoa1212793
 22. Menon BK, Smith EE, Modi J, Patel SK, Bhatia R, Watson TW, Hill MD, Demchuk AM, Goyal M (2011) Regional leptomeningeal score on CT angiography predicts clinical and imaging outcomes in patients with acute anterior circulation occlusions. *AJNR Am J Neuroradiol* 32(9):1640–1645. doi:10.3174/ajnr.A2564
 23. Liebeskind DS, Tomsick TA, Foster LD, Yeatts SD, Carrozzella J, Demchuk AM, Jovin TG, Khatri P, von Kummer R, Sugg RM, Zaidat OO, Hussain SI, Goyal M, Menon BK, Al Ali F, Yan B, Palesch YY, Broderick JP, Investigators II (2014) Collaterals at angiography and outcomes in the interventional management of stroke (IMS) III trial. *Stroke* 45(3):759–764. doi:10.1161/STROKEAHA.113.004072
 24. Nambiar V, Sohn SI, Almekhlafi MA, Chang HW, Mishra S, Qazi E, Eesa M, Demchuk AM, Goyal M, Hill MD, Menon BK (2014) CTA collateral status and response to recanalization in patients with acute ischemic stroke. *AJNR Am J Neuroradiol* 35(5):884–890. doi:10.3174/ajnr.A3817
 25. Fiehler J, Kucinski T, Knudsen K, Rosenkranz M, Thomalla G, Weiller C, Rother J, Zeumer H (2004) Are there time-dependent differences in diffusion and perfusion within the first 6 hours after stroke onset? *Stroke* 35(9):2099–2104. doi:10.1161/01.STR.0000138450.15078.b5
 26. Copen WA, Rezai Gharai L, Barak ER, Schwamm LH, Wu O, Kamalian S, Gonzalez RG, Schaefer PW (2009) Existence of the diffusion-perfusion mismatch within 24 hours after onset of acute stroke: dependence on proximal arterial occlusion. *Radiology* 250(3):878–886. doi:10.1148/radiol.2503080811
 27. Sorensen AG, Copen WA, Ostergaard L, Buonanno FS, Gonzalez RG, Rordorf G, Rosen BR, Schwamm LH, Weisskoff RM, Koroshetz WJ (1999) Hyperacute stroke: simultaneous measurement of relative cerebral blood volume, relative cerebral blood flow, and mean tissue transit time. *Radiology* 210(2):519–527. doi:10.1148/radiology.210.2.r99fe06519
 28. Neumann-Haefelin T, Wittsack HJ, Wenserski F, Siebler M, Seitz RJ, Modder U, Freund HJ (1999) Diffusion- and perfusion-weighted MRI. The DWI/PWI mismatch region in acute stroke. *Stroke* 30(8):1591–1597

29. Darby DG, Barber PA, Gerraty RP, Desmond PM, Yang Q, Parsons M, Li T, Tress BM, Davis SM (1999) Pathophysiological topography of acute ischemia by combined diffusion-weighted and perfusion MRI. *Stroke* 30(10):2043–2052
30. Gonzalez RG, Hakimelahi R, Schaefer PW, Roccatagliata L, Sorensen AG, Singhal AB (2010) Stability of large diffusion/perfusion mismatch in anterior circulation strokes for 4 or more hours. *BMC Neurol* 10:13. doi:10.1186/1471-2377-10-13
31. Hakimelahi R, Vachha BA, Copen WA, Papini GD, He J, Higazi MM, Lev MH, Schaefer PW, Yoo AJ, Schwamm LH, Gonzalez RG (2014) Time and diffusion lesion size in major anterior circulation ischemic strokes. *Stroke* 45(10):2936–2941. doi:10.1161/STROKEAHA.114.005644
32. Campbell BC, Christensen S, Levi CR, Desmond PM, Donnan GA, Davis SM, Parsons MW (2012) Comparison of computed tomography perfusion and magnetic resonance imaging perfusion-diffusion mismatch in ischemic stroke. *Stroke* 43(10):2648–2653. doi:10.1161/STROKEAHA.112.660548
33. Lin L, Bivard A, Levi CR, Parsons MW (2014) Comparison of computed tomographic and magnetic resonance perfusion measurements in acute ischemic stroke: back-to-back quantitative analysis. *Stroke* 45(6):1727–1732. doi:10.1161/STROKEAHA.114.005419
34. Qiao Y, Zhu G, Patrie J, Xin W, Michel P, Eskandari A, Jovin T, Wintermark M (2014) Optimal perfusion computed tomographic thresholds for ischemic core and penumbra are not time dependent in the clinically relevant time window. *Stroke* 45(5):1355–1362. doi:10.1161/STROKEAHA.113.003362
35. Sztrihai LK, Cusack U, Kandasamy N, Jarosz J, Kalra L (2013) Determinants of mismatch in acute ischaemic stroke. *J Neurol Sci* 334(1–2):10–13. doi:10.1016/j.jns.2013.07.002
36. Campbell BC, Christensen S, Tress BM, Churilov L, Desmond PM, Parsons MW, Barber PA, Levi CR, Bladin C, Donnan GA, Davis SM (2013) Failure of collateral blood flow is associated with infarct growth in ischemic stroke. *J Cereb Blood Flow Metab* 33(8):1168–1172. doi:10.1038/jcbfm.2013.77
37. Miteff F, Levi CR, Bateman GA, Spratt N, McElduff P, Parsons MW (2009) The independent predictive utility of computed tomography angiographic collateral status in acute ischaemic stroke. *Brain* 132(Pt 8):2231–2238. doi:10.1093/brain/awp155
38. Shuaib A, Butcher K, Mohammad AA, Saqqur M, Liebeskind DS (2011) Collateral blood vessels in acute ischaemic stroke: a potential therapeutic target. *Lancet Neurol* 10(10):909–921. doi:10.1016/S1474-4422(11)70195-8
39. Zhang H, Prabhakar P, Sealock R, Faber JE (2010) Wide genetic variation in the native pial collateral circulation is a major determinant of variation in severity of stroke. *J Cereb Blood Flow Metab* 30(5):923–934. doi:10.1038/jcbfm.2010.10
40. Beyer SE, von Baumgarten L, Thierfelder KM, Rottenkolber M, Janssen H, Dichgans M, Johnson TR, Straube A, Ertl-Wagner B, Reiser MF, Sommer WH (2014) Predictive value of the velocity of collateral filling in patients with acute ischemic stroke. *J Cereb Blood Flow Metab*. doi:10.1038/jcbfm.2014.182
41. Kucinski T, Koch C, Eckert B, Becker V, Kromer H, Heesen C, Grzyska U, Freitag HJ, Rother J, Zeumer H (2003) Collateral circulation is an independent radiological predictor of outcome after thrombolysis in acute ischaemic stroke. *Neuroradiology* 45(1):11–18. doi:10.1007/s00234-002-0881-0
42. Christoforidis GA, Mohammad Y, Kehagias D, Avutu B, Slivka AP (2005) Angiographic assessment of pial collaterals as a prognostic indicator following intra-arterial thrombolysis for acute ischemic stroke. *AJNR Am J Neuroradiol* 26(7):1789–1797
43. Maas MB, Lev MH, Ay H, Singhal AB, Greer DM, Smith WS, Harris GJ, Halpern E, Kemmling A, Koroshetz WJ, Furie KL (2009) Collateral vessels on CT angiography predict outcome in acute ischemic stroke. *Stroke* 40(9):3001–3005. doi:10.1161/STROKEAHA.109.552513
44. Jung S, Gilgen M, Slotboom J, El-Koussy M, Zubler C, Kiefer C, Luedi R, Mono ML, Heldner MR, Weck A, Mordasini P, Schroth G, Mattle HP, Arnold M, Gralla J, Fischer U (2013) Factors that determine penumbral tissue loss in acute ischaemic stroke. *Brain* 136(Pt 12):3554–3560. doi:10.1093/brain/awt246
45. Kamalian S, Kamalian S, Maas MB, Goldmacher GV, Payabvash S, Akbar A, Schaefer PW, Furie KL, Gonzalez RG, Lev MH (2011) CT cerebral blood flow maps optimally correlate with admission diffusion-weighted imaging in acute stroke but thresholds vary by postprocessing platform. *Stroke* 42(7):1923–1928. doi:10.1161/strokeaha.110.610618
46. Bivard A, Levi C, Spratt N, Parsons M (2013) Perfusion CT in acute stroke: a comprehensive analysis of infarct and penumbra. *Radiology* 267(2):543–550. doi:10.1148/radiol.12120971

VI Lebenslauf

Christine Theresia Bollwein

Geboren am 09.05.1990 in Schwandorf

Seit 07/2016 Assistenzärztin für Pathologie am Pathologischen Institut der TU München

Ausbildung	2016	3. Abschnitt der Ärztlichen Prüfung, München Approbation mit der Note 1,0
	2015 - 2016	Praktisches Jahr
	2015	2. Abschnitt der Ärztlichen Prüfung, München
	2011	1. Abschnitt der Ärztlichen Prüfung, München
	2000 - 2009	Carl-Friedrich-Gauß Gymnasium Schwandorf Abitur mit der Note 1,3

Praktisches Jahr

Dezember 2015 – April 2016	Klinikum Fürstenfeldbruck, Anästhesiologie
September 2015 – Dezember 2015	Zentralklinikum Augsburg, Chirurgie
Mai 2015 – September 2015	RoMed Klinikum Rosenheim, Innere Medizin

Famulaturen

Unfallchirurgie	Februar/März 2012	Helios Klinik Titisee-Neustadt
Allgemeinmedizin	August/September 2012	Gemeinschaftspraxis Wittmann/Pollinger/Michl, Bruck, Oberpfalz
Radiologie	September/Oktober 2013	Institut für klinische Radiologie, LMU, München
Kardiologie	März/April 2014	Herz- und Gefäßklinik GmbH, Bad Neustadt/Saale

VII Danksagung

An erster Stelle möchte ich mich bei meinem Doktorvater Prof. Dr. med. Wieland Sommer bedanken, der mir dieses interessante Promotionsthema zur Verfügung stellte. Von der Konzeption der Studien bis zum Verfassen der Manuskripte war er immer ein verlässlicher Ansprechpartner. Seine Expertise in statistischen Fragestellungen und im radiologischen Fachbereich war für die Erstellung der Dissertation eine wertvolle Hilfestellung.

Besonderer Dank gilt auch PD Dr. med. Louisa von Baumgarten für ihre Geduld bei der Korrektur der Manuskripte und ihre konstruktiven Anregungen und Ratschläge. PD Dr. med. Dipl. Wirt.-Inform. Kolja Thierfelder verdanke ich vor allem seine Unterstützung bei technischen und methodischen Fragestellungen.

Ebenso danken möchte ich all den Coautoren, die einen wesentlichen Beitrag zum Gelingen der Studien geleistet haben.

Zu guter Letzt danke ich meiner Familie für ihre vielfältige Unterstützung, ohne die ich das bisher Erreichte nie geschafft hätte. Meinem Freund Martin danke ich insbesondere für seine unermessliche Geduld, sein Verständnis und seine hilfreichen IT-Kenntnisse.

VIII Eidesstattliche Versicherung

Bollwein, Christine

Ich erkläre hiermit an Eides statt,
dass ich die vorliegende Dissertation zum Thema

Untersuchungen zur Rolle der Ganzhirn CT-Perfusion in der akuten Schlaganfalldiagnostik

selbstständig verfasst, mich außer der angegebenen keiner weiteren Hilfsmittel bedient und alle Erkenntnisse, die aus dem Schrifttum ganz oder annähernd übernommen sind, als solche kenntlich gemacht und nach ihrer Herkunft unter Bezeichnung der Fundstelle einzeln nachgewiesen habe.

Ich erkläre des Weiteren, dass die hier vorgelegte Dissertation nicht in gleicher oder in ähnlicher Form bei einer anderen Stelle zur Erlangung eines akademischen Grades eingereicht wurde.

München, 11.04.2018

Christine Bollwein

Ort, Datum

Unterschrift